UNIVERSITAT DE BARCELONA

Insights into the molecular mechanisms of apoptosis induced by glucose deprivation

Raffaella Iurlaro

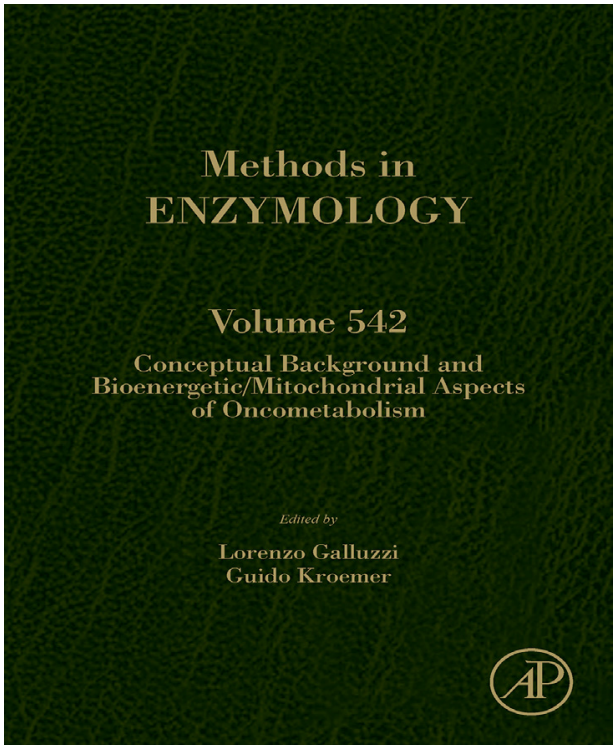

From: Raffaella Iurlaro, Clara Lucía León-Annicchiarico, Cristina Muñoz-Pinedo, Regulation of Cancer Metabolism by Oncogenes and Tumor Suppressors. In Lorenzo Galluzzi, Guido Kroemer editors: *Methods In Enzymology*, Vol. 542, Burlington: Academic Press, 2014, pp.59-80.
ISBN: 978-0-12-416618-9

CHAPTER THREE

Regulation of Cancer Metabolism by Oncogenes and Tumor Suppressors

Raffaella Iurlaro[1], Clara Lucía León-Annicchiarico[1], Cristina Muñoz-Pinedo[2]

Cell Death Regulation Group, Bellvitge Biomedical Research Institute (IDIBELL), Barcelona, Spain
[1]These authors contributed equally.
[2]Corresponding author: e-mail address: cmunoz@idibell.cat

Contents

1. Introduction 60
2. HIF-1: Regulator of Hypoxic Responses and Cancer Metabolism 61
3. The PI3K–AKT–PTEN Pathway Regulates Metabolism 62
4. mTOR Controls Anabolism and It Is Inhibited By AMPK Upon Metabolic Stress 64
5. c-Myc Promotes Aerobic Anabolism 66
6. Ras Stimulates Glycolysis and the PPP 68
7. NF-kappaB Regulates Inflammation and Proliferation But Also Metabolism 69
8. Retinoblastoma: Suppressing Tumorogenesis and Anabolism 70
9. p53 Regulates Multiple Metabolic Pathways 71
10. Conclusions 74
Acknowledgments 74
References 74

Abstract

Cell proliferation requires the coordination of multiple signaling pathways as well as the provision of metabolic substrates. Nutrients are required to generate such building blocks and their form of utilization differs to significant extents between malignant tissues and their nontransformed counterparts. Thus, oncogenes and tumor suppressor genes regulate the proliferation of cancer cells also by controlling their metabolism. Here, we discuss the central anabolic functions of the signaling pathways emanating from mammalian target of rapamycin, MYC, and hypoxia-inducible factor-1. Moreover, we analyze how oncogenic proteins like phosphoinositide-3-kinase, AKT, and RAS, tumor suppressors such as phosphatase and tensin homolog, retinoblastoma, and p53, as well as other factors associated with the proliferation or survival of cancer cells, such as NF-κB, regulate cellular metabolism.

Methods in Enzymology, Volume 542
ISSN 0076-6879
http://dx.doi.org/10.1016/B978-0-12-416618-9.00003-0

ABBREVIATIONS

AMPK AMP-activated protein kinase
COX cytochrome c oxidase
GLS1 glutaminase 1
HIF-1 hypoxia-inducible factor 1
IκB inhibitor of κB proteins
LDH lactate dehydrogenase
LKB1 liver kinase B1
mTOR mammalian (or mechanistic) target of rapamycin
PDH pyruvate dehydrogenase
PDK1 pyruvate dehydrogenase kinase 1
PHD prolyl-4-hydroxylase domain protein
pRb retinoblastoma protein
PtdIns(3,4,5) P3 phosphatidylinositol-3,4,5-trisphosphate
PTEN phosphatase and tensin homologue
SCO2 synthesis of cytochrome c oxidase 2
SREBP sterol regulatory element-binding protein
TIGAR TP53 (tumor protein 53)-induced glycolysis and apoptosis regulator
TSC1/2 tuberous sclerosis 1/2
VHL von Hippel–Lindau

1. INTRODUCTION

Most oncogenes and tumor suppressor genes encode proteins that promote cellular proliferation or cell cycle arrest. In recent years, we are learning that proliferation is tightly coupled with metabolic changes. For this reason, cancer metabolism is an area of intense research, since the metabolism of cancer cells can be exploited for therapeutic purposes (Munoz-Pinedo, El Mjiyad, & Ricci, 2012). In accordance to the normal function of their encoded proteins, oncogenes or tumor suppressors regulate cellular metabolism (Vander Heiden, Cantley, & Thompson, 2009). This is an intrinsic part of their program to reduce or promote cell proliferation. Oncogenes promote glucose and amino acid uptake and metabolism in order to make new lipids, nucleotides, and proteins. Conversely, tumor suppressors upregulate mitochondrial respiration and Krebs (TCA) cycle (see review by Frezza and colleagues, Chapter 1 of this volume). We will discuss how several oncogenes and tumor suppressors regulate cellular metabolism.

2. HIF-1: REGULATOR OF HYPOXIC RESPONSES AND CANCER METABOLISM

Highly proliferating tumor cells are characterized by a hypoxic microenvironment due to the increased oxygen consumption, which stimulates metabolic reprogramming (Vaupel, Thews, & Hoeckel, 2001). The master regulator of cellular responses to low oxygen is hypoxia-inducible factor 1 (HIF-1), a transcription factor induced by hypoxic conditions and whose levels are increased in many human cancers even under normoxia (Semenza, 2010). Under normal oxygen conditions, HIF-1 is degraded by the proteasome after prolyl hydroxylation by prolyl-4-hydroxylase domain proteins (PHDs) and ubiquitination by the tumor suppressor von Hippel–Lindau (VHL) (Kaelin & Ratcliffe, 2008; Fig. 3.1). HIF-1 can also be constitutively activated by genetic alterations, such as the loss of function of VHL in renal cancer cells, or due to the accumulation of metabolites such as fumarate or succinate (Boulahbel, Duran, & Gottlieb, 2009). Cancer cells frequently undergo oxygen shortage which inhibits the prolyl hydroxylases and stabilizes HIF-1, which induces the expression of hundreds of genes involved in angiogenesis, metabolism, apoptosis, and proliferation.

The major metabolic effect of HIF-1 is to trigger the switch from mitochondrial oxidative phosphorylation (OXPHOS) to anaerobic glycolysis. HIF-1 induces the expression of glucose transporters (GLUT-1, GLUT-3) to enhance glucose uptake and it upregulates glycolytic enzymes and the lactate dehydrogenase A (LDHA) subunit to stimulate the conversion of pyruvate into lactate (Brahimi-Horn, Chiche, & Pouyssegur, 2007; Semenza, 2011; Fig. 3.1). Importantly, HIF-1 activates the pyruvate dehydrogenase kinase 1 (PDK1; Kim, Tchernyshyov, Semenza, & Dang, 2006; McFate et al., 2008), a negative regulator of pyruvate dehydrogenase (PDH). PDH converts pyruvate into acetyl-CoA to enter the Krebs cycle in the mitochondria (Fig. 3.1). The effect of inhibiting PDH is the inhibition of mitochondrial oxygen consumption and reduction of ROS production, and this promotes anaerobic glycolysis and thus the Warburg effect (Papandreou, Cairns, Fontana, Lim, & Denko, 2006).

HIF-1 also controls respiration by regulating expression and stability of the cytochrome oxidase subunits cytochrome c oxidase (COX)4-1 and COX4-2 (Fukuda et al., 2007). Additionally, HIF-1 upregulates the expression of the proteins BNIP3 and BNIP3L, which trigger mitochondrial

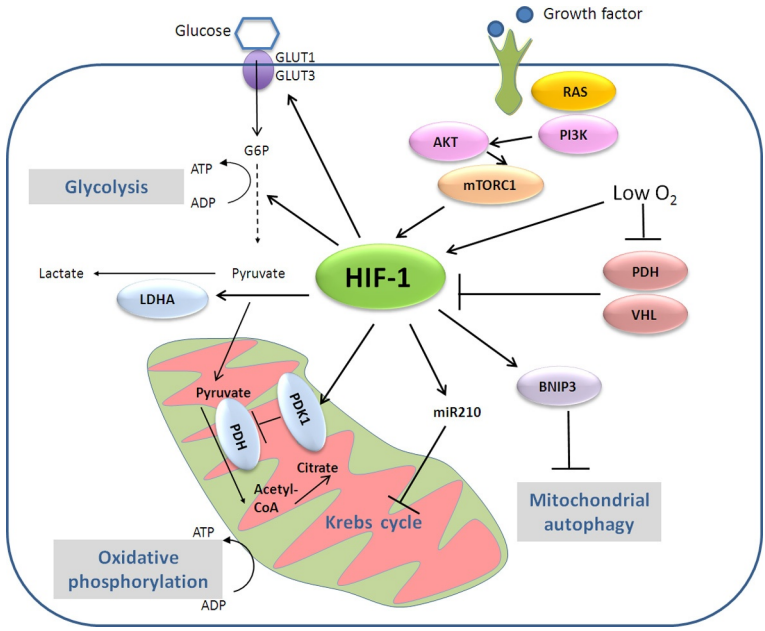

Figure 3.1 *Regulation of cancer metabolism by HIF-1*. HIF-1 switches metabolism from oxidative respiration to anaerobic glycolysis. Hypoxia induces HIF-1 by blocking its inhibitors prolyl-4-hydroxylase domain proteins (PHDs) and von Hippel–Lindau (VHL) protein that need O_2 to exert their functions. Once activated, HIF-1 upregulates the glucose transporters GLUT1 and GLUT3, thus enhancing glucose uptake. HIF-1 induces the expression of almost every enzyme of the glycolytic pathway and lactate dehydrogenase A (LDHA), thus resulting in lactate production. Importantly, HIF-1 induces the pyruvate dehydrogenase kinase 1 (PDK1) that phosphorylates pyruvate dehydrogenase (PDH) blocking the entry of pyruvate into the mitochondria. HIF-1 also induces the expression of miR210, inhibiting important enzymes of Krebs cycle, and upregulates the protein BNIP3 that promotes mitochondrial autophagy.

autophagy, another possible mechanism by which HIF-1 reduces oxidative metabolism (Zhang et al., 2008). HIF-1 can also activate the transcription of miR-210, a microRNA which blocks the expression or activity of some enzymes of the Krebs cycle and the Complex I of the electron transport chain (Chen, Li, Zhang, Huang, & Luthra, 2010; Favaro et al., 2010; Fig. 3.1).

3. THE PI3K–AKT–PTEN PATHWAY REGULATES METABOLISM

The PI3K–AKT pathway is one of the main prosurvival pathways activated in human cancers. The phosphatidylinositol 3-kinases (PI3Ks) are a

family of proteins that phosphorylate phoshoinositides at the D-3 position of the inositol ring, and their functions are linked to different biological roles, like regulation of cell growth, organismal metabolism, cell proliferation, and vesicle trafficking (Cantley, 2002; Engelman, Luo, & Cantley, 2006).

The best known effector downstream of PI3K is AKT (also known as Protein Kinase B, PKB). Oncogenic mutations in PI3K increase the PI3K and AKT signaling, promoting factor-independent growth and increasing cell invasion and metastasis (Manning & Cantley, 2007). Activated AKT is also an important driver of oncogenic metabolism. It was recognized early that AKT activation drives the glycolytic metabolism of tumor cells (Fig. 3.2; Elstrom et al., 2004). Activation of AKT increases cellular glucose uptake by inducing the expression and membrane translocation of glucose transporters (Barthel et al., 1999; Kohn, Summers, Birnbaum, & Roth, 1996). AKT also

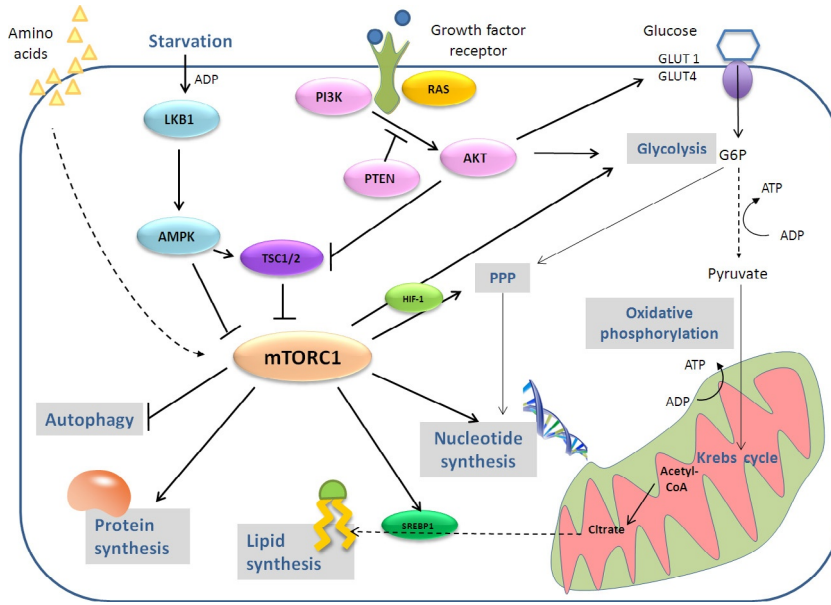

Figure 3.2 *Regulation of cancer metabolism by the PI3K–AKT–PTEN and LKB1–AMPK–mTORC1 pathways.* Growth factor receptors activate Ras and phosphatidylinositol 3-kinase (PI3K) leading to the activation of AKT. Once activated, AKT induces glycolysis by regulating glycolytic enzymes and glucose transporters. These effects are counteracted by the phosphatase and tensin homologue (PTEN). AKT can indirectly activate the mTORC1 pathway that promotes lipid, protein, and nucleotide synthesis, contributing to the building of bioblocks necessary for tumor proliferation. Under stress conditions, the AMP-activated protein kinase (AMPK) activation through the liver kinase B1 (LKB1), opposes glycolytic metabolism in part by inhibiting mTORC1. PPP, pentose phosphate pathway.

increases glycolysis by activating the enzyme phosphofructokinase-1 (PFK1) through phosphorylation of phosphofructokinase-2 (PFK2) (Deprez, Vertommen, Alessi, Hue, & Rider, 1997), which leads to allosteric activation of PFK1. In addition, AKT stimulates the mammalian (or mechanistic) target of rapamycin (mTOR) pathway, thus promoting many other metabolic branches as we will discuss below.

PI3K/AKT signaling pathway can be inhibited by the tumor suppressor gene phosphatase and tensin homologue (PTEN). PTEN dephosphorylates phosphatidylinositol-3,4,5-trisphosphate (PtdIns(3,4,5) P3), the second messenger generated by the activation of PI3K, and the main activator of AKT, thereby inhibiting the PI3K–AKT–mTOR pathway. The main functions of PTEN are the regulation of cell growth, metabolism, and survival, and thus it has an important tumor-suppressive ability (Carracedo & Pandolfi, 2008). Even a slight decrease of PTEN levels, or a fine change in *PTEN* gene expression, is sufficient to induce cancer susceptibility (Alimonti et al., 2010). Consistently, loss of PTEN promotes glycolysis (Tandon et al., 2011) and elevation of PTEN levels can reverse the cancer metabolic reprogramming from glycolysis to OXPHOS (Garcia-Cao et al., 2012). For example, transgenic mice carrying additional copies of *PTEN* (referred to as Super-PTEN mice), are less prone to cancer development. In this model, PTEN elevation resulted in a healthier metabolism, with systemic metabolic reprogramming; mice display increased oxygen consumption and energy expenditure, higher mitochondrial biogenesis increasing the mitochondrial ATP production, and an important reduction of body fat accumulation. Cells derived from these mice show reduced glucose and glutamine uptake, increased mitochondrial OXPHOS, and resistance to oncogenic transformation (Garcia-Cao et al., 2012). Conversely, in nontransformed thyrocytes of a PTEN-deficient mouse model, the constitutive PTEN deficiency caused a downregulation of Krebs cycle and OXPHOS, defective mitochondria and reduction of respiration with compensatory glycolysis. In this case, the metabolic switch to glycolysis is driven by PI3K-dependent AMP-activated protein kinase (AMPK) inactivation (Antico Arciuch, Russo, Kang, & Di Cristofano, 2013).

4. mTOR CONTROLS ANABOLISM AND IT IS INHIBITED BY AMPK UPON METABOLIC STRESS

mTOR is a serine/threonine kinase that is part of two distinct complexes, TORC1 and TORC2, which have different sensitivity to rapamycin. We will discuss the role of the rapamycin sensitive complex,

mTORC1, which controls cell growth and metabolism in response to environmental signals (Wullschleger, Loewith, & Hall, 2006). The mTOR pathway is one of the most deregulated signaling pathways in human cancer, and growth-factor-independent activation of mTORC1 is observed in up to 80% of tumors, across nearly all lineages (Guertin & Sabatini, 2007; Menon & Manning, 2009). mTOR is also deregulated in metabolic disorders, such as obesity and type 2 diabetes. Mice with hyperactive mTORC1 signaling in the liver display metabolic abnormalities, including defects in glucose and lipid homeostasis, and subsequently develop hepatocellular carcinoma (Menon et al., 2012).

mTOR integrates diverse signals to regulate cell growth: growth factors, nutrients, oxygen, energy, and several forms of stress. mTOR, downstream of PI3K, responds to growth factors via the inactivation of tuberous sclerosis (TSC)1 and TSC2 by AKT; these proteins are negative regulators of mTORC1 (Manning & Cantley, 2007; Fig. 3.2). Nutrients, particularly amino acids, also regulate mTORC1 signaling, which controls protein translation. The molecular mechanism by which mTORC1 senses intracellular amino acids is not fully understood, but it requires the Rag GTPases (Kim, Goraksha-Hicks, Li, Neufeld, & Guan, 2008; Sancak et al., 2010).

mTOR regulates many anabolic pathways. Through regulation of HIF1 it activates glycolysis and the pentose phosphate pathway (PPP) (Figs. 3.1 and 3.2), and by activating the transcription factor sterol regulatory element-binding protein (SREBP)1, it also stimulates lipid synthesis (Düvel et al., 2010; Fig. 3.2). Nucleotide synthesis is also regulated by mTOR in two different manners: through regulation of the PPP and by activation of an enzyme of pyrimidine synthesis (Ben-Sahra, Howell, Asara, & Manning, 2013; Robitaille et al., 2013). Thus, cells with active mTOR are stimulated to proliferate by making all necessary building blocks.

mTOR is inhibited in conditions of nutritional stress by the AMPK. Tumors under metabolic stress adapt to these conditions by altering the liver kinase B1 (LKB1)–AMPK pathway (Sebbagh, Olschwang, Santoni, & Borg, 2011). As a result, the LKB1–AMPK pathway works as a metabolic checkpoint and inhibits cancer metabolic reprogramming (Jones et al., 2005; Kuhajda, 2008). AMPK is an ATP sensor that checks and regulates cellular energy homeostasis. AMPK is activated in response to nutrient deprivation or hypoxia, when ATP levels decline and the AMP and ADP levels increase (Fig. 3.2) (Hardie, 2011; Xiao et al., 2011). Under conditions of energy stress, LKB1 (serine–threonine kinase LKB1) acts as the main upstream kinase that activates AMPK (Shaw, Bardeesy, et al., 2004; Woods et al.,

2003). Once activated, AMPK can target a wide range of downstream metabolic pathways, especially the mTOR pathway. During energetic stress, AMPK can inhibit mTORC1 through two different mechanism; phosphorylating TSC2 (Corradetti, Inoki, Bardeesy, DePinho, & Guan, 2004; Inoki, Zhu, & Guan, 2003; Shaw, Kosmatka, et al., 2004) or by direct phosphorylation of Raptor, a component of mTORC1 (Scott, Norman, Hawley, Kontogiannis, & Hardie, 2002). LKB1-deficient cells and mutant mice for LKB1, or MEFs deficient for TSC2, show hyperactive mTORC1 signaling in response to energy stress (Shaw, Bardeesy, et al., 2004). Thus, AMPK alters important cellular responses, like cell growth, proliferation and autophagy (Shackelford et al., 2009). The lack of AMPK signaling increase tumorigenesis and enhances the glycolytic metabolism in cancer cells (Faubert et al., 2012). However, AMPK can also promote survival of tumor cells: LKB1 deficiency reduces the AMPK signaling in tumor cells (Godlewski et al., 2010; Shackelford & Shaw, 2009; Zheng et al., 2009), and deletion of LKB1 makes the cells more sensitive to nutrient deprivation (Shaw, Bardeesy, et al., 2004). Additionally, by inhibiting lipid synthesis and promoting lipid oxidation, AMPK contributes to maintenance of NADPH levels thus mitigating redox stress (Jeon, Chandel, & Hay, 2012).

5. c-MYC PROMOTES AEROBIC ANABOLISM

c-Myc has been reported to be the master regulator of metabolic processes involved in cell proliferation. Myc is deregulated in many human cancers in which it triggers tumorogenesis through the transcriptional modulation of many genes. In fact, it has been recently proposed that Myc is a "general" transcription factor, in the sense that high levels of c-Myc in tumor cells produce elevated levels of transcripts from the existing gene expression program of tumor cells (Lin et al., 2012). This includes genes involved in glucose metabolism, nucleotide, lipid, amino acid, and protein synthesis (Dang, 2013; Li & Simon, 2013). Once activated, c-Myc binds, with its cofactor Max, to the consensus sequences called "E-boxes" present in genes driven by all three RNA polymerases, resulting in ribosomal RNA synthesis and ribosome biogenesis, necessary to build the increasing cell mass (Grandori et al., 2005; van Riggelen, Yetil, & Felsher, 2010).

c-Myc also regulates mitochondrial biogenesis by inducing the expression of genes involved in mitochondrial structure and function, such as *TFAM* which encodes a protein involved in mitochondrial transcription and mitochondrial DNA replication (Li, 2005; Fig. 3.3). To trigger biomass

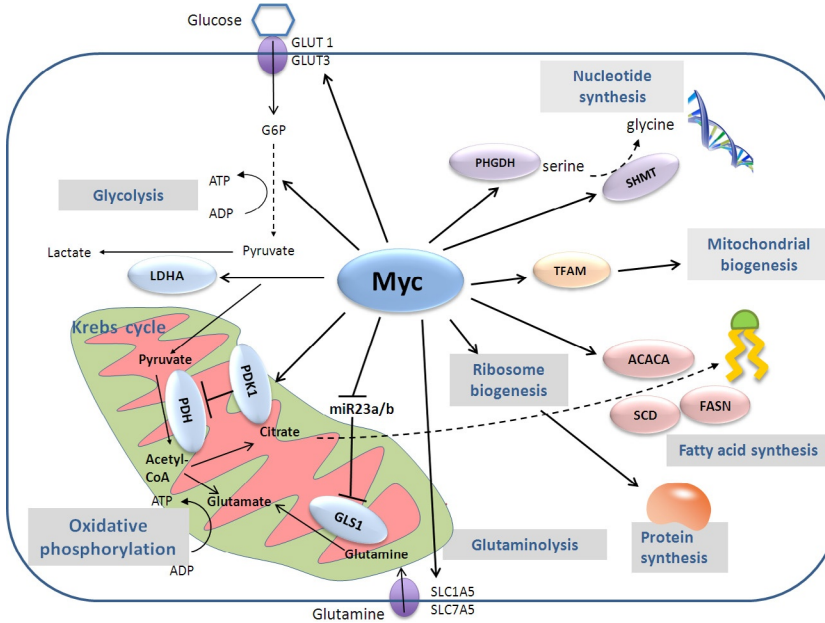

Figure 3.3 *Myc regulates cancer metabolism*. Myc promotes cancer cell metabolism at several levels. Myc upregulates the glucose transporters GLUT1 and GLUT3 increasing glucose uptake. It induces several glycolytic enzymes such as the lactate dehydrogenase A (LDHA) resulting in lactate production. Like HIF-1, Myc induces pyruvate dehydrogenase kinase 1 (PDK1) expression, which prevents pyruvate entry into the mitochondria. Myc also regulates glutaminolysis: it upregulates glutamine transporters SLC1A5 and SLC7A5 and induces glutaminase 1 (GLS1) expression. Myc also promotes biomass accumulation essential for proliferating tumor cells. It regulates ribosome biogenesis, mitochondrial biogenesis, and several enzymes involved in fatty acids synthesis such as acetyl-CoA carboxylase (ACACA), fatty acid synthetase (FASN), and stearoyl-CoA desaturase (SCD). Additionally, Myc regulates enzymes involved in nucleotide synthesis such as phosphoglycerate dehydrogenase (PHGDH) and serine hydroxymethyltransferase (SHMT).

accumulation necessary for cell proliferation, c-Myc induces the expression of almost every glycolytic gene, redirecting cells to glucose consumption for ATP but also for biomolecule production. c-Myc also stimulates the transcription of LDHA that is necessary for c-Myc mediated tumorigenesis in some models (Shim et al., 1997; Fig. 3.3).

Like HIF-1, c-Myc regulates other important glycolytic enzymes such as hexokinase 2 -that phosphorylates glucose to make glucose-6-phosphate- and PDK1 -which phosphorylates and inhibits PDH, blocking the entry of pyruvate into the mitochondria (Kim, Gao, Liu, Semenza, & Dang,

2007; Fig. 3.3). It has been shown by *in vivo* imaging techniques that in c-Myc-driven liver tumors pyruvate is converted preferentially to lactate (Hu et al., 2011). Interestingly, metabolic changes were detected prior to the appearance of tumors: in pretumor tissues, an accumulation of alanine due to increased expression of transaminases was observed.

c-Myc also controls glutamine metabolism, achieved through regulation of mitochondrial glutaminase 1 (GLS1) expression (Gao et al., 2009). Glutamine is converted to glutamate by GLS1, whose expression is increased in c-Myc-dependent tumors. Glutamate then enters the Krebs cycle to produce ATP or glutathione. There are evidences that GLS1 is regulated by c-Myc also at posttranscriptional level. c-Myc suppresses the expression of two miRNAs, miR-23a and miR-23b, which target GLS1 in its 3′UTR, resulting in increased glutaminase expression and glutamine metabolism. c-Myc also stimulates the transport of glutamine inside the cell by increasing the expression of the glutamine transporters SLC1A5 and SLC7A5 (Fig. 3.3).

It has been shown that c-Myc can regulate nucleotide biosynthesis by transcriptional regulation of several key enzymes, redirecting glycolysis to the synthesis of serine and glycine that are essential for nucleotide building (Mannava et al., 2008). Recently, Myc has also been associated to lipid synthesis as many enzymes of fatty acid biosynthesis are its direct targets and they contribute to the building of bioblocks needed in the c-Myc-driven proliferation program (Loven et al., 2012; Fig. 3.3). Thus, Myc has been shown to activate all pathways necessary to build new cells.

6. RAS STIMULATES GLYCOLYSIS AND THE PPP

The Ras family encompasses a number of small GTPases that transduce signals to induce proliferation, including the metabolic switch. Transfection of a constitutively activated form of Ras is sufficient to stimulate glycolysis and the PPP (Vizan et al., 2005). Ras proteins are activated downstream of growth factors or they are constitutively active in tumors, and they signal through MAP kinases and/or through PI3K. Some of the metabolic effects of Ras, thus, may be mediated through the PI3K/AKT/mTOR pathway, while other effects can be due to stimulation of Myc. H-Ras, for instance, upregulates Glut-1 mRNA through the PI3-kinase pathway. This effect is indirect, through the PI3K-mediated upregulation of HIF-1 (Chen, Pore, Behrooz, Ismail-Beigi, & Maity, 2001). Since Ras can indirectly regulate HIF-1, it can regulate metabolism in the same manner,

and this is for instance the case in colon cancer cells with hyperactivated KRas, in which KRas inhibits mitochondrial metabolism through activation of HIF-1 (Chun et al., 2010).

Pancreatic tumors often carry activating KRAS mutations. In these cells, KRas regulates multiple metabolic pathways at the transcriptional level. It stimulates glucose uptake and it channels glucose intermediates into the hexosamine biosynthesis and PPPs. These effects are mediated by MAP kinases and Myc (Ying et al., 2012). Additionally, pancreatic ductal adenocarcinomas have recently been shown to depend on a nonclassical glutamine utilization pathway stimulated transcriptionally by Kras. Kras directs the metabolism of these cells in toward the use of glutamine as a source of pyruvate and NADPH to maintain the cellular redox balance (Son et al., 2013).

Ras is also a regulator of autophagy, a cellular process that can provide nutrients by self-digestion of intracellular components. This process is also responsible for clearance of damaged mitochondria. Ras-mediated transformation induces autophagy, which is required to maintain mitochondrial metabolic functions in Ras-driven tumors (Guo et al., 2011). In these tumors, knockdown of essential autophagy genes can promote the accumulation of abnormal mitochondria unable to metabolize lipids through fatty acid oxidation (White, 2013). Similarly, tumors driven by a Ras downstream effector, the oncogene BRAF, rely on autophagy to maintain healthy mitochondria and glutamine metabolism (Strohecker et al., 2013).

7. NF-kappaB REGULATES INFLAMMATION AND PROLIFERATION BUT ALSO METABOLISM

NF-κB is a transcription factor of the Rel-homology-domain family. Its subunit p65/RelA is the most important in transactivation of several target genes involved in immunity, inflammation, and proliferation. Its activity is tightly regulated by the inhibitors of κB proteins (IκBs) and the IκB kinase proteins (IKKs), and it results in the expression of growth factors, cytokines, and promotion of cell proliferation (Hayden & Ghosh, 2004). Although NF-κB is not considered a classical oncogene, its expression can be regulated by several oncogenes, suggesting a role of NF-κB in promotion of tumorogenesis (Basseres & Baldwin, 2006). It has been reported that oncogenic H-Ras activates NF-κB (Finco et al., 1997) inducing lung tumor progression *in vivo* in a p53-dependent (Meylan et al., 2009) or independent manner (Bassères, Ebbs, Levantini, & Baldwin, 2010). In cells with mutated

p53, the activation of Ras induces a metabolic switch from oxidative mitochondrial phosphorylation to aerobic glycolysis that has been related to NF-κB activation (Kawauchi, Araki, Tobiume, & Tanaka, 2008). In this model, the loss of p53 activity resulted in transcriptional activation of NF-κB that was essential for the enhanced glucose consumption and lactate production. GLUT3 expression was directly regulated by NF-κB, accordingly with the observed increase of glucose uptake in those cells. Recently, it has been shown that NF-κB activation by the epidermal growth factor receptor (EGFR) in cancer cells induces the expression of pyruvate kinase M2 (PKM2), triggering lactate production and glucose uptake (Yang et al., 2012). However, NF-κB has also been shown to contribute to tumorogenesis by sustaining mitochondrial function. This effect was mediated through p53 and its target synthesis of cytochrome c oxidase 2 (SCO2), which increases OXPHOS (Mauro et al., 2011). Although NF-κB is not a typical oncogene, all these findings suggest an involvement of NF-κB in metabolic reprogramming and tumorigenesis. However, the manner by which NF-κB regulates cancer metabolism is still unclear and may be context dependent.

8. RETINOBLASTOMA: SUPPRESSING TUMOROGENESIS AND ANABOLISM

The retinoblastoma protein (pRb) is one of the tumor suppressors whose role in cancer metabolism has been most extensively studied (Nicolay & Dyson, 2013). The major function of pRb is the inhibition of cell cycle progression exerted through repression of the E2F1 transcription factor. This function is reverted by pRb phosphorylation by cyclin D-CDK4/6, which inactivates Rb and promotes E2F1-mediated transcription. Many signals can regulate pRb expression; among those, AMPK has been shown to phosphorylate directly pRb controlling the G1/S phase transition based on the energy status of the cell (Dasgupta & Milbrandt, 2009). Recently, pRb was shown to regulate starvation-induced stress response in *Caenorhabditis elegans* (Cui, Cohen, Teng, & Han, 2013) and similar results have been recently provided in a Drosophila model, suggesting an involvement of pRb in cancer metabolism (Nicolay et al., 2013). This study shows that flies with mutant RBF1 (Drosophila Rb homolog) are hypersensitive to fasting conditions and present deregulated glutamine and nucleotide metabolism. Also human cancers with inactivated pRb show an increase in glutamine uptake due to upregulation of expression of the glutamine

transporter ASCT2, and an increase in glutamine utilization in the Krebs cycle resulting in glutathione accumulation (Reynolds et al., 2014). pRb and E2F1 can regulate in an opposite way the oxidative metabolism, modulating the expression of different genes at their promoters. pRb deletion in murine erythrocytes causes a block in differentiation and impairs mitochondrial biogenesis uncovering a positive role of pRb on mitochondrial activity (Sankaran, Orkin, & Walkley, 2008), while other studies show that E2F1 induces a switch from oxidative to glycolytic metabolism by repressing multiple genes involved in mitochondrial function (Blanchet et al., 2011). Some studies have described a role of pRb in lipid metabolism, showing that pRb deletion induces E2F-dependent expression of fatty acid biosynthesis enzymes and SREBP (Shamma et al., 2009). Additionally, pRb has been shown to play a role in nucleotide metabolism by inhibiting enzymes such as dihydrofolate reductase and thymidylate synthase (Angus et al., 2002). All these data indicate a connection of pRb in cell cycle progression and regulation of tumor metabolism.

9. p53 REGULATES MULTIPLE METABOLIC PATHWAYS

p53 function is lost in most human cancers (Soussi & Beroud, 2001). p53 exerts an important defense mechanism against tumor development (Vousden & Ryan, 2009). It is a transcription factor that regulates a large range of functions like DNA damage response, apoptosis, and senescence. Mutations in p53 found in tumors can produce a variety of biological effects, for example: lack of control in cell cycle, defective apoptosis, and inefficient DNA repair (Resnick & Inga, 2003). In p53 knockout mice, tumor development is rapid and spontaneous (Donehower et al., 1992). p53 also plays an important role in metabolic stress response (Vousden & Ryan, 2009). Cells lacking p53 and deprived of glucose cannot undergo cell cycle arrest, since p53 controls a metabolic checkpoint. This makes p53-defective cells more sensitive than nontransformed cells to metabolic stress, what has led to propose the use of antiglycolytic drugs for therapy of p53-deficient tumors (Jones et al., 2005). p53 also responds to lack of serine and allows *de novo* synthesized serine to be channeled to production of reduced glutathione to counter oxidative stress (Maddocks et al., 2013). For this reason, p53-deficient cells are more sensitive to serine depletion.

As part of the antitumor activity of p53, it promotes glucose OXPHOS and it inhibits glycolysis (Fig. 3.4). Disruption of TP53 in mice promotes a significant decrease in oxygen consumption that closely correlates with p53

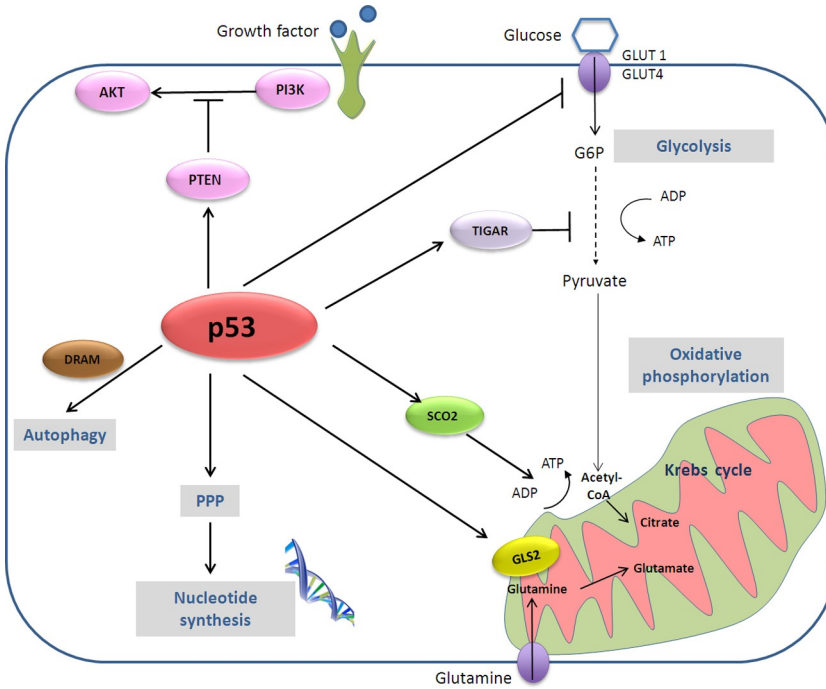

Figure 3.4 *p53 regulates multiple metabolic pathways*. p53 responds to metabolic stress and it can inhibit the tumorigenic metabolic switch by suppressing glycolysis and activating the phosphatase and tensin homologue (PTEN). p53 inhibits the transcription of GLUT1 and GLUT4 reducing glucose uptake and it upregulates the TP53 (tumor protein 53)-induced glycolysis and apoptosis regulator (TIGAR), which results in glycolysis inhibition. p53 increases the mitochondrial metabolism by activation of the synthesis of cytochrome c oxidase 2 (SCO2), thus promoting oxidative phosphorylation. p53 can also induce, contradictorily, prosurvival responses in cancer cells, for instance when it increases the flux through the pentose phosphate pathway (PPP) or glutamine utilization. P53 can regulate positively autophagy by increasing the expression of DRAM.

deficiency, as p53 increases OXPHOS through upregulation of the gene SCO2, whose product participates in the assembly of COX in the mitochondria (Matoba et al., 2006). p53 upregulates TP53-induced glycolysis and apoptosis regulator (TIGAR), an enzyme that decreases the levels of the glycolytic activator fructose-2,6-bisphosphate (Bensaad et al., 2006). It also inhibits glucose uptake by inhibiting the transcription of GLUT1 and GLUT4 (Schwartzenberg-Bar-Yoseph, Armoni, & Karnieli, 2004). p53 can also inhibit the glycolytic pathway indirectly by activating PTEN, thus inhibiting the PI3K pathway (Stambolic et al., 2001).

p53 is also involved in somewhat contradictory responses, since it has been associated with pathways that may support tumor growth and survival. For example, in some tumor cells it can increase the flux through the PPP, reducing oxidative stress and promoting anabolism, thus helping the growth of cancer cells (Vousden & Ryan, 2009). p53 is also able to contribute to glutaminolysis, an alternative fuel bioenergetic pathway, where glutamine is metabolized to produce α-ketoglutarate from glutamate in the Krebs cycle. This pathway is important in the process of oncogenic transformation: the enzyme which converts glutamine to glutamate, glutaminase 1 (GLS1/KGA) has been shown to help tumor development (Wang et al., 2010). p53 can play a role in the regulation of glutaminolysis by the activation of another isoform of glutaminase (GLS2/LGA), helping the cells produce ATP in periods of glucose deprivation (Hu et al., 2010; Suzuki et al., 2010). Both the activation of the PPP and glutaminolysis could have a function in reduction of oxidative stress.

Another function of p53 is related to autophagy. The control of p53 in autophagy is context specific, and it could work like a prodeath or cell survival mechanism. One of the ways by which p53 regulates autophagy is by upregulating damage regulated autophagy modulator (DRAM), a lysosomal protein that positively regulates autophagy (Crighton et al., 2006).

The family of transcription factors of p53 includes p63 and p73, both functional homologs with high sequential and structural similarity (Kaghad et al., 1997; Yang et al., 1998). These two members of the p53 family have functions that are markedly different from those of p53 (Allocati et al., 2012), but they also have many similarities and overlapping activity with p53, including the regulation of cellular metabolism (Berkers, Maddocks, Cheung, Mor, & Vousden, 2013). Tp63 and Tp73 genes are transcribed from two different promoters, and the final product can be either full length proteins that retain a full transactivation (TA) domain (TAp63 and TAp73) or N-terminally truncated isoforms (ΔNp63 and ΔNp73) (De Laurenzi & Melino, 2000). TAp63 can control fat and glucose metabolism, because is a positive regulator of the transcription of Sirt1, AMPKa2, and LKB1. TAp73 can promote cancer cell proliferation, controlling biosynthetic pathways and cellular antioxidant capacity through the regulation of glucose metabolism. TAp73 regulates the expression of glucose-6-phosphate dehydrogenase (G6PD), an enzyme involved in glucose metabolism through the PPP (Du et al., 2013). p73 can be negatively regulated by AMPKα by direct interaction without affecting p53, which represses the TAp73 transcription program (Lee, Lee, Sin, Kim, & Um, 2008).

And recently it was discovered that like p53, TAp73 is implicated in the maintenance of mitochondrial Complex IV (Rufini et al., 2012).

In summary, p53 opposes the PI3K pathway to inhibit anabolism, it promotes mitochondrial metabolism and it regulates oxidative stress. The metabolic roles of p53 may well be more important for its tumor suppressor abilities than its roles as a proapoptotic or prosenescent proteins, as recently revealed by a study employing a mutant that had lost these functions and still suppressed tumorogenesis (Li et al., 2012).

10. CONCLUSIONS

To date, a good number of oncogenes and tumor suppressors have been shown to play a role as regulators of metabolism. The vast literature is growing quickly, and we have only summarized here the roles of a few of these genes. However, many other proteins involved in cancer have been shown to play roles in metabolism, from the breast cancer associated receptor tyrosine kinase ErbB2 (Her2/neu) (Zhao et al., 2009) to the promyelocytic leukemia tumor suppressor (Carracedo et al., 2012) or many of the Bcl-2 family of antiapoptotic proteins (reviewed by Fulda and colleagues, Chapter 4 of this volume). Metabolic rewiring is such an important part of the cellular growth process that we will likely see this field expanding in the future.

ACKNOWLEDGMENTS

Studies in CMP's lab related to the topic of this review are supported by FIS grant PI13/00139. R. I. is supported by a fellowship of SUR of the ECO of the Government of Catalonia. We apologize to colleagues whose work could not be cited.

REFERENCES

Alimonti, A., Carracedo, A., Clohessy, J. G., Trotman, L. C., Nardella, C., & Egia, A. (2010). Subtle variations in Pten dose determine cancer susceptibility. *Nature Genetics*, *42*(5), 454–458.

Allocati, N., Di Ilio, C., & De Laurenzi, V. (2012). p63/p73 in the control of cell cycle and cell death. *Experimental Cell Research*, *318*(11), 1285–1290.

Angus, S. P., Wheeler, L. J., Ranmal, S. A., Zhang, X., Markey, M. P., & Mathews, C. K. (2002). Retinoblastoma tumor suppressor targets dNTP metabolism to regulate DNA replication. *Journal of Biological Chemistry*, *277*(46), 44376–44384. http://dx.doi.org/10.1074/jbc.M205911200.

Antico Arciuch, V. G., Russo, M. A., Kang, K. S., & Di Cristofano, A. (2013). Inhibition of AMPK and Krebs cycle gene expression drives metabolic remodeling of Pten-deficient preneoplastic thyroid cells. *Cancer Research*, *73*(17), 5459–5472.

Barthel, A., Okino, S. T., Liao, J., Nakatani, K., Li, J., & Whitlock, J. P., Jr. (1999). Regulation of GLUT1 gene transcription by the serine/threonine kinase Akt1. *The Journal of Biological Chemistry*, *274*(29), 20281–20286.

Basseres, D. S., & Baldwin, A. S. (2006). Nuclear factor-[kappa]B and inhibitor of [kappa]B kinase pathways in oncogenic initiation and progression. *Oncogene*, *25*(51), 6817.

Bassères, D. S., Ebbs, A., Levantini, E., & Baldwin, A. S. (2010). Requirement of the NF-kappaB subunit p65/RelA for K-Ras-induced lung tumorigenesis. *Cancer Research*, *70*(9), 3537–3546. http://dx.doi.org/10.1158/0008-5472.can-09-4290.

Bensaad, K., Tsuruta, A., Selak, M. A., Vidal, M. N., Nakano, K., & Bartrons, R. (2006). TIGAR, a p53-inducible regulator of glycolysis and apoptosis. *Cell*, *126*(1), 107–120.

Ben-Sahra, I., Howell, J. J., Asara, J. M., & Manning, B. D. (2013). Stimulation of de novo pyrimidine synthesis by growth signaling through mTOR and S6K1. *Science*, *339*(6125), 1323–1328.

Berkers, C. R., Maddocks, O. D., Cheung, E. C., Mor, I., & Vousden, K. H. (2013). Metabolic regulation by p53 family members. *Cell Metabolism*, *18*(5), 617–633.

Blanchet, E., Annicotte, J.-S., Lagarrigue, S., Aguilar, V., Clape, C., & Chavey, C. (2011). E2F transcription factor-1 regulates oxidative metabolism. *Nature Cell Biology*, *13*(9), 1146.

Boulahbel, H., Duran, R. V., & Gottlieb, E. (2009). Prolyl hydroxylases as regulators of cell metabolism. *Biochemical Society Transactions*, *37*(Pt 1), 291–294. http://dx.doi.org/10.1042/BST0370291, BST0370291 [pii].

Brahimi-Horn, M. C., Chiche, J., & Pouyssegur, J. (2007). Hypoxia signalling controls metabolic demand. *Current Opinion in Cell Biology*, *19*(2), 223.

Cantley, L. C. (2002). The phosphoinositide 3-kinase pathway. *Science*, *296*(5573), 1655–1657.

Carracedo, A., & Pandolfi, P. P. (2008). The PTEN–PI3K pathway: Of feedbacks and cross-talks. *Oncogene*, *27*(41), 5527–5541.

Carracedo, A., Weiss, D., Leliaert, A. K., Bhasin, M., de Boer, V. C., & Laurent, G. (2012). A metabolic prosurvival role for PML in breast cancer. *The Journal of Clinical Investigation*, *122*(9), 3088–3100.

Chen, Z., Li, Y., Zhang, H., Huang, P., & Luthra, R. (2010). Hypoxia-regulated microRNA-210 modulates mitochondrial function and decreases ISCU and COX10 expression. *Oncogene*, *29*(30), 4362.

Chen, C., Pore, N., Behrooz, A., Ismail-Beigi, F., & Maity, A. (2001). Regulation of glut1 mRNA by hypoxia-inducible factor-1. Interaction between H-ras and hypoxia. *The Journal of Biological Chemistry*, *276*, 9519.

Chun, S. Y., Johnson, C., Washburn, J. G., Cruz-Correa, M. R., Dang, D. T., & Dang, L. H. (2010). Oncogenic KRAS modulates mitochondrial metabolism in human colon cancer cells by inducing HIF-1alpha and HIF-2alpha target genes. *Molecular Cancer*, *9*, 293.

Corradetti, M. N., Inoki, K., Bardeesy, N., DePinho, R. A., & Guan, K.-L. (2004). Regulation of the TSC pathway by LKB1: Evidence of a molecular link between tuberous sclerosis complex and Peutz-Jeghers syndrome. *Genes & Development*, *18*(13), 1533–1538.

Crighton, D., Wilkinson, S., O'Prey, J., Syed, N., Smith, P., & Harrison, P. R. (2006). DRAM, a p53-induced modulator of autophagy, is critical for apoptosis. *Cell*, *126*(1), 121.

Cui, M., Cohen, M. L., Teng, C., & Han, M. (2013). The tumor suppressor Rb critically regulates starvation-induced stress response in C. elegans. *Current Biology*, *23*(11), 975.

Dang, C. V. (2013). MYC, metabolism, cell growth, and tumorigenesis. *Cold Spring Harbor Perspectives in Medicine*, *3*(8), a014217.

Dasgupta, B., & Milbrandt, J. (2009). AMP-activated protein kinase phosphorylates retinoblastoma protein to control mammalian brain development. *Developmental Cell*, *16*(2), 256.

De Laurenzi, V., & Melino, G. (2000). Evolution of functions within the p53/p63/p73 family. *Annals of the New York Academy of Sciences*, *926*, 90–100.

Deprez, J., Vertommen, D., Alessi, D. R., Hue, L., & Rider, M. H. (1997). Phosphorylation and activation of heart 6-phosphofructo-2-kinase by protein kinase B and other protein kinases of the insulin signaling cascades. *The Journal of Biological Chemistry*, *272*(28), 17269–17275.

Donehower, L. A., Harvey, M., Slagle, B. L., McArthur, M. J., Montgomery, C. A., Jr., & Butel, J. S. (1992). Mice deficient for p53 are developmentally normal but susceptible to spontaneous tumours. *Nature*, *356*(6366), 215–221.

Du, W., Jiang, P., Mancuso, A., Stonestrom, A., Brewer, M. D., & Minn, A. J. (2013). TAp73 enhances the pentose phosphate pathway and supports cell proliferation. *Nature Cell Biology*, *15*(8), 991–1000.

Düvel, K., Yecies, J. L., Menon, S., Raman, P., Lipovsky, A. I., & Souza, A. L. (2010). Activation of a metabolic gene regulatory network downstream of mTOR complex 1. *Molecular Cell*, *39*(2), 171.

Elstrom, R. L., Bauer, D. E., Buzzai, M., Karnauskas, R., Harris, M. H., & Plas, D. R. (2004). Akt stimulates aerobic glycolysis in cancer cells. *Cancer Research*, *64*(11), 3892–3899. http://dx.doi.org/10.1158/0008-5472.can-03-2904.

Engelman, J. A., Luo, J., & Cantley, L. C. (2006). The evolution of phosphatidylinositol 3-kinases as regulators of growth and metabolism. *Nature Reviews Genetics*, 7(8), 606–619.

Faubert, B., Boily, G., Izreig, S., Griss, T., Samborska, B., & Dong, Z. (2012). AMPK is a negative regulator of the Warburg effect and suppresses tumor growth in vivo. *Cell Metabolism*, *17*(1), 113–124.

Favaro, E., Ramachandran, A., McCormick, R., Gee, H., Blancher, C., & Crosby, M. (2010). MicroRNA-210 regulates mitochondrial free radical response to hypoxia and krebs cycle in cancer cells by targeting iron sulfur cluster protein ISCU. *PLoS One*, *5*(4), e10345. http://dx.doi.org/10.1371/journal.pone.0010345.

Finco, T. S., Westwick, J. K., Norris, J. L., Beg, A. A., Der, C. J., & Baldwin, A. S. (1997). Oncogenic Ha-Ras-induced signaling activates NF-kappaB transcriptional activity, which is required for cellular transformation. *Journal of Biological Chemistry*, *272*(39), 24113–24116. http://dx.doi.org/10.1074/jbc.272.39.24113.

Fukuda, R., Zhang, H., Kim, J. W., Shimoda, L., Dang, C. V., & Semenza, G. L. (2007). HIF-1 regulates cytochrome oxidase subunits to optimize efficiency of respiration in hypoxic cells. *Cell*, *129*(1), 111–122. http://dx.doi.org/10.1016/j.cell.2007.01.047, S0092-8674(07)00307-8 [pii].

Gao, P., Tchernyshyov, I., Chang, T.-C., Lee, Y.-S., Kita, K., & Ochi, T. (2009). c-Myc suppression of miR-23a/b enhances mitochondrial glutaminase expression and glutamine metabolism. *Nature*, *458*(7239), 762.

Garcia-Cao, I., Song, M. S., Hobbs, R. M., Laurent, G., Giorgi, C., & de Boer, V. C. (2012). Systemic elevation of PTEN induces a tumor-suppressive metabolic state. *Cell*, *149*(1), 49–62.

Godlewski, J., Nowicki, M. O., Bronisz, A., Nuovo, G., Palatini, J., & De Lay, M. (2010). MicroRNA-451 regulates LKB1/AMPK signaling and allows adaptation to metabolic stress in glioma cells. *Molecular Cell*, *37*(5), 620.

Grandori, C., Gomez-Roman, N., Felton-Edkins, Z. A., Ngouenet, C., Galloway, D. A., & Eisenman, R. N. (2005). c-Myc binds to human ribosomal DNA and stimulates transcription of rRNA genes by RNA polymerase I. *Nature Cell Biology*, 7(3), 311.

Guertin, D. A., & Sabatini, D. M. (2007). Defining the role of mTOR in cancer. *Cancer Cell*, *12*(1), 9.

Guo, J. Y., Chen, H. Y., Mathew, R., Fan, J., Strohecker, A. M., & Karsli-Uzunbas, G. (2011). Activated Ras requires autophagy to maintain oxidative metabolism and tumorigenesis. *Genes & Development*, *25*(5), 460–470.

Hardie, D. G. (2011). Adenosine monophosphate-activated protein kinase: A central regulator of metabolism with roles in diabetes, cancer, and viral infection. *Cold Spring Harbor Symposia on Quantitative Biology*, *76*, 155–164. http://dx.doi.org/10.1101/sqb.2011.76.010819.

Hayden, M. S., & Ghosh, S. (2004). Signaling to NF-KB. *Genes & Development*, *18*(18), 2195–2224. http://dx.doi.org/10.1101/gad.1228704.

Hu, S., Balakrishnan, A., Bok, R. A., Anderton, B., Larson, P. E. Z., & Nelson, S. J. (2011). 13C-Pyruvate imaging reveals alterations in glycolysis that precede c-Myc-induced tumor formation and regression. *Cell Metabolism*, *14*(1), 131–142.

Hu, W., Zhang, C., Wu, R., Sun, Y., Levine, A., & Feng, Z. (2010). Glutaminase 2, a novel p53 target gene regulating energy metabolism and antioxidant function. *Proceedings of the National Academy of Sciences of the United States of America*, *107*(16), 7455–7460.

Inoki, K., Zhu, T., & Guan, K.-L. (2003). TSC2 mediates cellular energy response to control cell growth and survival. *Cell*, *115*(5), 577.

Jeon, S. M., Chandel, N. S., & Hay, N. (2012). AMPK regulates NADPH homeostasis to promote tumour cell survival during energy stress. *Nature*, *485*(7400), 661–665.

Jones, R. G., Plas, D. R., Kubek, S., Buzzai, M., Mu, J., & Xu, Y. (2005). AMP-activated protein kinase induces a p53-dependent metabolic checkpoint. *Molecular Cell*, *18*(3), 283.

Kaelin, W. G., & Ratcliffe, P. J. (2008). Oxygen sensing by metazoans: The central role of the HIF hydroxylase pathway. *Molecular Cell*, *30*(4), 393.

Kaghad, M., Bonnet, H., Yang, A., Creancier, L., Biscan, J. C., & Valent, A. (1997). Monoallelically expressed gene related to p53 at 1p36, a region frequently deleted in neuroblastoma and other human cancers. *Cell*, *90*(4), 809–819.

Kawauchi, K., Araki, K., Tobiume, K., & Tanaka, N. (2008). p53 regulates glucose metabolism through an IKK-NF-[kappa]B pathway and inhibits cell transformation. *Nature Cell Biology*, *10*(5), 611.

Kim, J. W., Gao, P., Liu, Y. C., Semenza, G. L., & Dang, C. V. (2007). Hypoxia-inducible factor 1 and dysregulated c-Myc cooperatively induce vascular endothelial growth factor and metabolic switches hexokinase 2 and pyruvate dehydrogenase kinase 1. *Molecular and Cellular Biology*, *27*, 7381.

Kim, E., Goraksha-Hicks, P., Li, L., Neufeld, T. P., & Guan, K. L. (2008). Regulation of TORC1 by Rag GTPases in nutrient response. *Nature Cell Biology*, *10*(8), 935–945.

Kim, J. W., Tchernyshyov, I., Semenza, G. L., & Dang, C. V. (2006). HIF-1-mediated expression of pyruvate dehydrogenase kinase: A metabolic switch required for cellular adaptation to hypoxia. *Cell Metabolism*, *3*(3), 177–185.

Kohn, A. D., Summers, S. A., Birnbaum, M. J., & Roth, R. A. (1996). Expression of a constitutively active Akt Ser/Thr kinase in 3T3-L1 adipocytes stimulates glucose uptake and glucose transporter 4 translocation. *The Journal of Biological Chemistry*, *271*(49), 31372–31378.

Kuhajda, F. P. (2008). AMP-activated protein kinase and human cancer: Cancer metabolism revisited. *International Journal of Obesity*, *32*(Suppl. 4), S36–S41.

Lee, Y. G., Lee, S. W., Sin, H. S., Kim, E. J., & Um, S. J. (2008). Kinase activity-independent suppression of p73α by AMP-activated kinase α (AMPKα). *Oncogene*, *28*(7), 1040–1052.

Li, F. (2005). Myc stimulates nuclearly encoded mitochondrial genes and mitochondrial biogenesis. *Molecular and Cellular Biology*, *25*, 6225.

Li, T., Kon, N., Jiang, L., Tan, M., Ludwig, T., & Zhao, Y. (2012). Tumor suppression in the absence of p53-mediated cell-cycle arrest, apoptosis, and senescence. *Cell*, *149*(6), 1269–1283.

Li, B., & Simon, M. C. (2013). Molecular Pathways: Targeting MYC-induced Metabolic Reprogramming and Oncogenic Stress in Cancer. *Clinical Cancer Research*, *19*(21), 5835–5841.

Lin, C. Y., Loven, J., Rahl, P. B., Paranal, R. M., Burge, C. B., & Bradner, J. E. (2012). Transcriptional amplification in tumor cells with elevated c-Myc. *Cell*, *151*(1), 56–67. http://dx.doi.org/10.1016/j.cell.2012.08.026, S0092-8674(12)01057-4 [pii].

Loven, J., Orlando, D. A., Sigova, A. A., Lin, C. Y., Rahl, P. B., & Burge, C. B. (2012). Revisiting global gene expression analysis. *Cell*, *151*(3), 476.

Maddocks, O. D., Berkers, C. R., Mason, S. M., Zheng, L., Blyth, K., & Gottlieb, E. (2013). Serine starvation induces stress and p53-dependent metabolic remodelling in cancer cells. *Nature*, *493*(7433), 542–546. http://dx.doi.org/10.1038/nature11743, nature11743 [pii].

Mannava, S., Grachtchouk, V., Wheeler, L. J., Im, M., Zhuang, D., & Slavina, E. G. (2008). Direct role of nucleotide metabolism in C-MYC-dependent proliferation of melanoma cells. *Cell Cycle*, *7*(15), 2392.

Manning, B. D., & Cantley, L. C. (2007). AKT/PKB signaling: Navigating downstream. *Cell*, *129*(7), 1261–1274.

Matoba, S., Kang, J.-G., Patino, W. D., Wragg, A., Boehm, M., & Gavrilova, O. (2006). p53 regulates mitochondrial respiration. *Science*, *312*(5780), 1650–1653. http://dx.doi.org/10.1126/science.1126863.

Mauro, C., Leow, S. C., Anso, E., Rocha, S., Thotakura, A. K., & Tornatore, L. (2011). NF-kappaB controls energy homeostasis and metabolic adaptation by upregulating mitochondrial respiration. *Nature Cell Biology*, *13*(10), 1272–1279. http://dx.doi.org/10.1038/ncb2324, ncb2324 [pii].

McFate, T., Mohyeldin, A., Lu, H., Thakar, J., Henriques, J., Halim, N. D., & Verma, A. (2008). Pyruvate dehydrogenase complex activity controls metabolic and malignant phenotype in cancer cells. *The Journal of Biological Chemistry*, *283*(33), 22700–22708.

Menon, S., & Manning, B. D. (2009). Common corruption of the mTOR signaling network in human tumors. *Oncogene*, *27*(S2), S43.

Menon, S., Yecies, J. L., Zhang, H. H., Howell, J. J., Nicholatos, J., & Harputlugil, E. (2012). Chronic activation of mTOR complex 1 is sufficient to cause hepatocellular carcinoma in mice. *Science Signaling*, *5*(217), ra24.

Meylan, E., Dooley, A. L., Feldser, D. M., Shen, L., Turk, E., & Ouyang, C. (2009). Requirement for NF-[kgr]B signalling in a mouse model of lung adenocarcinoma. *Nature*, *462*(7269), 104.

Munoz-Pinedo, C., El Mjiyad, N., & Ricci, J. E. (2012). Cancer metabolism: Current perspectives and future directions. *Cell Death and Disease*, *3*, e248.

Nicolay, B. N., & Dyson, N. J. (2013). The multiple connections between pRB and cell metabolism. *Current Opinion in Cell Biology*, *25*(6), 735–740.

Nicolay, B. N., Gameiro, P. A., Tschöp, K., Korenjak, M., Heilmann, A. M., & Asara, J. M. (2013). Loss of RBF1 changes glutamine catabolism. *Genes & Development*, *27*(2), 182–196. http://dx.doi.org/10.1101/gad.206227.112.

Papandreou, I., Cairns, R. A., Fontana, L., Lim, A. L., & Denko, N. C. (2006). HIF-1 mediates adaptation to hypoxia by actively downregulating mitochondrial oxygen consumption. *Cell Metabolism*, *3*(3), 187–197.

Resnick, M. A., & Inga, A. (2003). Functional mutants of the sequence-specific transcription factor p53 and implications for master genes of diversity. *Proceedings of the National Academy of Sciences of the United States of America*, *100*(17), 9934–9939.

Reynolds, M. R., Lane, A. N., Robertson, B., Kemp, S., Liu, Y., Hill, B. G., et al. (2014). Control of glutamine metabolism by the tumor suppressor Rb. *Oncogene*, *33*(5), 556–566.

Robitaille, A. M., Christen, S., Shimobayashi, M., Cornu, M., Fava, L. L., & Moes, S. (2013). Quantitative phosphoproteomics reveal mTORC1 activates de novo pyrimidine synthesis. *Science*, *339*(6125), 1320–1323. http://dx.doi.org/10.1126/science.1228771, science.1228771, [pii].

Rufini, A., Niklison-Chirou, M. V., Inoue, S., Tomasini, R., Harris, I. S., & Marino, A. (2012). TAp73 depletion accelerates aging through metabolic dysregulation. *Genes & Development*, *26*(18), 2009–2014.

Sancak, Y., Bar-Peled, L., Zoncu, R., Markhard, A. L., Nada, S., & Sabatini, D. M. (2010). Ragulator-Rag complex targets mTORC1 to the lysosomal surface and is necessary for its activation by amino acids. *Cell*, *141*(2), 290–303.

Sankaran, V. G., Orkin, S. H., & Walkley, C. R. (2008). Rb intrinsically promotes erythropoiesis by coupling cell cycle exit with mitochondrial biogenesis. *Genes & Development*, *22*(4), 463–475. http://dx.doi.org/10.1101/gad.1627208.

Schwartzenberg-Bar-Yoseph, F., Armoni, M., & Karnieli, E. (2004). The tumor suppressor p53 down-regulates glucose transporters GLUT1 and GLUT4 gene expression. *Cancer Research*, *64*(7), 2627–2633.

Scott, J. W., Norman, D. G., Hawley, S. A., Kontogiannis, L., & Hardie, D. G. (2002). Protein kinase substrate recognition studied using the recombinant catalytic domain of AMP-activated protein kinase and a model substrate. *Journal of Molecular Biology*, *317*(2), 309–323.

Sebbagh, M., Olschwang, S., Santoni, M. J., & Borg, J. P. (2011). The LKB1 complex-AMPK pathway: The tree that hides the forest. *Familial Cancer*, *10*(3), 415–424.

Semenza, G. L. (2010). Defining the role of hypoxia-inducible factor 1 in cancer biology and therapeutics. *Oncogene*, *29*(5), 625–634.

Semenza, G. L. (2011). Regulation of metabolism by hypoxia-inducible factor 1. *Cold Spring Harbor Symposia on Quantitative Biology*, *76*, 347–353. http://dx.doi.org/10.1101/sqb.2011.76.010678.

Shackelford, D. B., & Shaw, R. J. (2009). The LKB1-AMPK pathway: Metabolism and growth control in tumour suppression. *Nature Reviews. Cancer*, *9*(8), 563.

Shackelford, D. B., Vasquez, D. S., Corbeil, J., Wu, S., Leblanc, M., & Wu, C. L. (2009). mTOR and HIF-1alpha-mediated tumor metabolism in an LKB1 mouse model of Peutz-Jeghers syndrome. *Proceedings of the National Academy of Sciences of the United States of America*, *106*(27), 11137–11142.

Shamma, A., Takegami, Y., Miki, T., Kitajima, S., Noda, M., & Obara, T. (2009). Rb regulates DNA damage response and cellular senescence through E2F-dependent suppression of N-Ras isoprenylation. *Cancer Cell*, *15*(4), 255.

Shaw, R. J., Bardeesy, N., Manning, B. D., Lopez, L., Kosmatka, M., & DePinho, R. A. (2004). The LKB1 tumor suppressor negatively regulates mTOR signaling. *Cancer Cell*, *6*(1), 91–99.

Shaw, R. J., Kosmatka, M., Bardeesy, N., Hurley, R. L., Witters, L. A., & DePinho, R. A. (2004). The tumor suppressor LKB1 kinase directly activates AMP-activated kinase and regulates apoptosis in response to energy stress. *Proceedings of the National Academy of Sciences of the United States of America*, *101*(10), 3329–3335.

Shim, H., Dolde, C., Lewis, B. C., Wu, C. S., Dang, G., & Jungmann, R. A. (1997). c-Myc transactivation of LDH-A: Implications for tumor metabolism and growth. *Proceedings of the National Academy of Sciences of the United States of America*, *94*(13), 6658–6663.

Son, J., Lyssiotis, C. A., Ying, H., Wang, X., Hua, S., & Ligorio, M. (2013). Glutamine supports pancreatic cancer growth through a KRAS-regulated metabolic pathway. *Nature*, *496*(7443), 101.

Soussi, T., & Beroud, C. (2001). Assessing TP53 status in human tumours to evaluate clinical outcome. *Nature Reviews. Cancer*, *1*(3), 233–240.

Stambolic, V., MacPherson, D., Sas, D., Lin, Y., Snow, B., & Jang, Y. (2001). Regulation of PTEN transcription by p53. *Molecular Cell*, *8*(2), 317–325.

Strohecker, A. M., Guo, J. Y., Karsli-Uzunbas, G., Price, S. M., Chen, G. J., Mathew, R., et al. (2013). Autophagy sustains mitochondrial glutamine metabolism and growth of BRAFV600E-driven lung tumors. *Cancer Discovery*, *3*(11), 1272–1285.

Suzuki, S., Tanaka, T., Poyurovsky, M. V., Nagano, H., Mayama, T., & Ohkubo, S. (2010). Phosphate-activated glutaminase (GLS2), a p53-inducible regulator of glutamine metabolism and reactive oxygen species. *Proceedings of the National Academy of Sciences of the United States of America*, *107*(16), 7461–7466.

Tandon, P., Gallo, C. A., Khatri, S., Barger, J. F., Yepiskoposyan, H., & Plas, D. R. (2011). Requirement for ribosomal protein S6 kinase 1 to mediate glycolysis and apoptosis resistance induced by Pten deficiency. *Proceedings of the National Academy of Sciences of the United States of America*, *108*(6), 2361–2365.

Vander Heiden, M. G., Cantley, L. C., & Thompson, C. B. (2009). Understanding the Warburg effect: The metabolic requirements of cell proliferation. *Science*, *324*(5930), 1029–1033.

van Riggelen, J., Yetil, A., & Felsher, D. W. (2010). MYC as a regulator of ribosome biogenesis and protein synthesis. *Nature Reviews. Cancer*, *10*(4), 301.

Vaupel, P., Thews, O., & Hoeckel, M. (2001). Treatment resistance of solid tumors: Role of hypoxia and anemia. *Medical Oncology*, *18*(4), 243–259. http://dx.doi.org/10.1385/MO:18:4:243, MO:18:4:243 [pii].

Vizan, P., Boros, L. G., Figueras, A., Capella, G., Mangues, R., & Bassilian, S. (2005). K-ras codon-specific mutations produce distinctive metabolic phenotypes in NIH3T3 mice [corrected] fibroblasts. *Cancer Research*, *65*(13), 5512–5515.

Vousden, K. H., & Ryan, K. M. (2009). p53 and metabolism. *Nature Reviews. Cancer*, *9*(10), 691.

Wang, J. B., Erickson, J. W., Fuji, R., Ramachandran, S., Gao, P., & Dinavahi, R. (2010). Targeting mitochondrial glutaminase activity inhibits oncogenic transformation. *Cancer Cell*, *18*(3), 207–219.

White, E. (2013). Exploiting the bad eating habits of Ras-driven cancers. *Genes & Development*, *27*(19), 2065–2071. http://dx.doi.org/10.1101/gad.228122.113, 27/19/2065 [pii].

Woods, A., Johnstone, S. R., Dickerson, K., Leiper, F. C., Fryer, L. G., & Neumann, D. (2003). LKB1 is the upstream kinase in the AMP-activated protein kinase cascade. *Current Biology*, *13*(22), 2004–2008.

Wullschleger, S., Loewith, R., & Hall, M. N. (2006). TOR signaling in growth and metabolism. *Cell*, *124*(3), 471–484.

Xiao, B., Sanders, M. J., Underwood, E., Heath, R., Mayer, F. V., & Carmena, D. (2011). Structure of mammalian AMPK and its regulation by ADP. *Nature*, *472*(7342), 230–233.

Yang, A., Kaghad, M., Wang, Y., Gillett, E., Fleming, M. D., & Dötsch, V. (1998). p63, a p53 homologue at 3q27-29, encodes multiple products with transactivating, deathinducing, and dominant-negative activities. *Molecular Cell*, *2*(3), 305–316.

Yang, W., Xia, Y., Cao, Y., Zheng, Y., Bu, W., & Zhang, L. (2012). EGFR-induced and PKCε monoubiquitylation-dependent NF-kappaB activation upregulates PKM2 expression and promotes tumorigenesis. *Molecular Cell*, *48*(5), 771.

Ying, H., Kimmelman, A. C., Lyssiotis, C. A., Hua, S., Chu, G. C., & Fletcher-Sananikone,-E. (2012). Oncogenic Kras maintains pancreatic tumors through regulation of anabolic glucose metabolism. *Cell*, *149*(3), 656.

Zhang, H., Bosch-Marce, M., Shimoda, L. A., Tan, Y. S., Baek, J. H., & Wesley, J. B. (2008). Mitochondrial autophagy is an HIF-1-dependent adaptive metabolic response to hypoxia. *Journal of Biological Chemistry*, *283*(16), 10892–10903. http://dx.doi.org/10.1074/jbc.M800102200.

Zhao, Y. H., Zhou, M., Liu, H., Ding, Y., Khong, H. T., & Yu, D. (2009). Upregulation of lactate dehydrogenase A by ErbB2 through heat shock factor 1 promotes breast cancer cell glycolysis and growth. *Oncogene*, *28*(42), 3689–3701.

Zheng, B., Jeong, J. H., Asara, J. M., Yuan, Y. Y., Granter, S. R., & Chin, L. (2009). Oncogenic B-RAF negatively regulates the tumor suppressor LKB1 to promote melanoma cell proliferation. *Molecular Cell*, *33*(2), 237–247.

OPEN

Citation: Cell Death and Disease (2014) 5, e1275; doi:10.1038/cddis.2014.237

www.nature.com/cddis

Apolipoprotein L2 contains a BH3-like domain but it does not behave as a BH3-only protein

J Galindo-Moreno[1], R Iurlaro[1], N El Mjiyad[1], J Díez-Pérez[2,3], T Gabaldón[2,3,4] and C Muñoz-Pinedo*[,1]

Apolipoproteins of the L family are lipid-binding proteins whose function is largely unknown. Apolipoprotein L1 and apolipoprotein L6 have been recently described as novel pro-death BH3-only proteins that are also capable of regulating autophagy. In an in-silico screening to discover novel putative BH3-only proteins, we identified yet another member of the apolipoprotein L family, apolipoprotein L2 (ApoL2), as a BH3 motif-containing protein. ApoL2 has been suggested to behave as a BH3-only protein and mediate cell death induced by interferon-gamma or viral infection. As previously described, we observed that ApoL2 protein was induced by interferon-gamma. However, knocking down its expression in HeLa cells did not regulate cell death induced by interferon-gamma. Overexpression of ApoL2 did not induce cell death on its own. ApoL2 did not sensitize or protect cells from overexpression of the BH3-only proteins Bmf or Noxa. Furthermore, siRNA against ApoL2 did not alter sensitivity to a variety of death stimuli. We could, however, detect a weak interaction between ApoL2 and Bcl-2 by immunoprecipitation of the former, suggesting a role of ApoL2 in a Bcl-2-regulated process like autophagy. However, in contrast to what has been described about its homologs ApoL1 and ApoL6, ApoL2 did not regulate autophagy. Thus, the role, if any, of ApoL2 in cell death remains to be clarified.

Cell Death and Disease (2014) **5,** e1275; doi:10.1038/cddis.2014.237; published online 5 June 2014
Subject Category: Immunity

Bcl-2 family proteins regulate mitochondrial permeability to control apoptosis. These proteins induce or inhibit cell death, and they are associated with a growing number of pathologies, including cancer and immune diseases.[1,2] For this reason, the search of new members of this family is of crucial importance. A subfamily of Bcl-2 homologs termed 'BH3-only proteins' comprises a growing number of proteins that only share a small motif of 15–21 amino acid residues.[3,4] This region, known as the 'BH3-domain', is essential for the apoptotic function of Bcl-2 family proteins. The homology in this region is relatively loose, and only a few residues are conserved among the members of the family. For this reason, BH3-only proteins have been identified by functional means rather than by sequence homology.

To identify novel BH3-only proteins we used a bioinformatics approach known as profile-based homology search. In brief, we constructed a so-called Hidden Markov Model (HMM) of the BH3-domain from the alignment of a set of proteins known to bear this domain. This HMM describes the probabilities of finding a given amino acid at a given position of the domain. This probabilistic model is then used to search in a sequence database for proteins that are likely to encode the same domain.

One of the proteins identified by this method was the apolipoprotein L2 (ApoL2). Two other members of this family, ApoL1 and ApoL6 have been described to behave as proapoptotic BH3-only proteins.[5–7] Although the functions of these proteins are still unclear, proteins of this family have been shown to bind lipids and they have been suggested to work as pore-forming proteins in intracellular membranes, based on the ability of ApoL1 to form pores in the lysosomal membrane of trypanosomes.[8,9] ApoL2 is highly homologous to ApoL1, and its BH3-like domain is very similar to those of ApoL1 and ApoL6. For these reasons, we explored the function of ApoL2 as a putative new BH3-only protein.

Results

Identification of novel BH3-containing proteins by using a profile-based homology search. Profile-based searches with profiles of BH3 domains as defined in ProSite[10] and PFAM,[11] as well as regular expression searches with motifs defined in the literature failed to provide satisfactory results in terms of specificity and sensitivity of detecting known human BH3 proteins (Table 1). Therefore, to efficiently identify novel putative BH3-only proteins, we collected the sequences of all human and mouse BH3 motifs annotated in Uniprot as well as those described in the literature, and aligned them to subsequently build an HMM for the BH3-domain (see Materials and Methods) (Figure 1a). This HMM provided better results in finding known BH3 than existing profiles at Pfam (Table 1), and was therefore used to search for

[1]Cell Death Regulation Group, IDIBELL (Institut d'Investigació Biomèdica de Bellvitge), Gran Via de L'Hospitalet 199, L'Hospitalet, 08908 Barcelona, Spain; [2]Comparative Genomics Group, Centre for Genomics Regulation, Dr. Aiguader, 88, 08003 Barcelona, Spain; [3]Universitat Pompeu Fabra (UPF), 08003 Barcelona, Spain and [4]Institució Catalana de Recerca i Estudis Avançats (ICREA), Pg. Lluís Companys 23, 08010 Barcelona, Spain
*Corresponding author: C Muñoz-Pinedo, IDIBELL – Hospital Duran i Reynals 3a planta, Gran Via de L'Hospitalet 199, L'Hospitalet, 08908 Barcelona, Spain. Tel: +34 93 260 7130; Fax: +34 93 260 7426; E-mail: cmunoz@idibell.cat
Keywords: apolipoproteins L; Bcl-2 family proteins; BH3-only; interferon-gamma; autophagy
Abbreviations: ApoL, apolipoprotein L; FBS, fetal bovine serum; IFN-γ, interferon-gamma; TNF, tumor necrosis factor
Received 22.1.14; revised 14.4.14; accepted 22.4.14; Edited by G Melino

putative novel BH3-containing proteins in the human proteome and genome.

Our screening identified BFK, a known Bcl-2 homolog originally left out from the list of proteins used to build the model,[12] and PXT1, a protein that has been recently described as a BH3-only protein that kills HeLa cells in a manner dependent of its BH3 motif[13] (Table 2). Another protein identified by this screening was the apolipoprotein L2 protein (Figure 1b, Table 2). Two apolipoproteins of the L family, ApoL1 and ApoL6, have been previously identified as BH3-only proteins.[5–7] ApoL2, due to its homology with ApoL1 and ApoL6 has indeed been proposed to be a BH3-only protein.[14] ApoL2 mRNA is ubiquitously expressed, according to the database IST Online (Supplementary Figure 1). We checked that this protein is expressed in a variety of cell lines of different origins (Figure 2a), and highly expressed in HeLa cervical cancer cell line, as predicted due to its high expression in cervical cancer.[15] ApoL2 is localized in HeLa cells outside the nucleus in a punctate state (Figure 2b) and it is not secreted (Figure 2c). Although it had been predicted to interact with membranes,[16] we observed that it did not colocalize with mitochondrial, endoplasmic reticulum or lysosomal markers (Figure 2b).

ApoL2 is transcriptionally induced by interferon-gamma in a number of non-transformed tissues.[14] In human bronchial epithelial cells its downregulation sensitized cells to cell death induced by IFN-γ, indicating that ApoL2 is an antiapoptotic protein in this context.[14] We observed that in HeLa cells IFN-γ induces ApoL2 (Figure 2d). However, when we downregulated ApoL2 using two different silencing sequences, we could not observe sensitization to cell death (Figure 2e).

Table 1 Summary of the results obtained from direct motif searches in the human proteome when using different strategies

Motif search	Hits in human proteome	Known BCL's (TP)	Sensitivity (TP/TP + FN)
1. Youle *et al.*[4]	5908	13	68.4%
2. Liu *et al.*[7]	152	16	84.2%
3. Prosite	28	9	47.36%
4. Novel HMM	26	19	100%

First column indicates the search strategy: using a direct search with (1) The consensus BH3 motif (LXXXGD) as defined in Youle *et al.*[4] (2) The extended motif (LXXX[GAS][DE]) used by Liu *et al.*[7] in their identification of Apol6; (3) The motif defined by Prosite[10] as of December 2008; and (4) an HMM-based search with the profile derived in this work. The following columns indicate, respectively, the number of total hits in the human proteome (Ensembl42 version), the number of known Bcl-2 family members identified of a total of 19 human members described in Youle *et al.*[4] and Uniprot (2008), and, finally the sensitivity of the search as computed by dividing the total number of correctly identified Bcl-2 family members (TP) by the total number of known Bcl-2 family members (TP + FN = 19). TP and FN stand for True Positives and False Negatives, respectively

ApoL2 is not a proapoptotic BH3-only protein. To check whether ApoL2 behaves as a proapoptotic Bcl-2 family member, we overexpressed ApoL2 in HeLa cells. Overexpression was confirmed by immunofluorescence (Supplementary Figure 2) and western blot (Supplementary Figure 3). We used Noxa and Bmf as proapoptotic BH3-only proteins, and verified that these proteins killed HeLa cells (Figure 3a). However, ApoL2 did not. We observed a trend of lower background death in cells overexpressing ApoL2, suggesting that ApoL2 is an antiapoptotic Bcl-2 family protein. To test this we overexpressed ApoL2 in combination with Noxa or Bmf. Our results indicate that ApoL2 confers a minor protection from Noxa (Figure 3a). However, this did not

b

Protein	UniProt ID	BH3 motive sequence
Bim	O43521	IAQE**L**RRIG**D**EFNAY
Bad	Q92934	YGRE**L**RRMS**D**EFVDS
Puma	Q9BXH1	IGAQ**L**RRMA**D**DLNAQ
Noxa	Q13794	CATQ**L**RRFG**D**KLNFR
Bcl-Rambo	Q9BXK5	MEDC**L**AHLG**E**KVSQE
Beclin-1	Q14457	LSRR**L**KVTG**D**LFDIM
ApoL6	Q9BWW8	NIDK**L**RALA**D**DIDKT
ApoL1	O14791	NIRR**L**RALA**D**GVQKV
ApoL2	Q9BQE5	HIRK**L**RALA**E**EVEQV

Figure 1 ApoL2 contains a BH3-like motif. (**a**) Logo representation of the protein profile used in the search for new BH3-domain proteins. The logo indicates the probability of finding a given amino acid at each of the 15 positions of the BH3-domain. Amino acids are represented by the one-letter code, and their height is proportional to the probability of appearing at a given position in the BH3-domain. (**b**) Alignment of ApoL2 BH3 motif with other BH3 motifs

Table 2 Summary of the putative BH3-only proteins predicted using HMM

Name	UniProt ID	NM ID	Amino acid number	Ensembl ID
Apolipoprotein L2 (ApoL2)	Q9BQE5	NM_030882.2 and NM_145637.1	337	ENSG00000128335
Arf-GAP with coiled-coil, ANK repeat and PH domain-containing protein 3 (ACAP3)	Q96P50	NM_030649.2	834	ENSG00000131584
GDP-fucose protein O-fucosyltransferase 2 (POFUT2)	Q9Y2G5	NM_015227.4	429	ENSG00000186866
Phenylalanine-4-hydroxylase(PHA)	P00439	NM_000277.1	452	ENSG00000171759
Peroxisomal testis-specific protein 1 (PXT1)	J3KR74	NM_152990.3	134	ENSG00000179165
Uncharacterized protein C19orf55 (C19orf55)	Q2NL68	NM_001039887	480 (putative)	ENSG00000167595

The table shows the different identification codes of the gene from the major databases. Uniprot ID (http://www.uniprot.org/), NM ID (http://www.ncbi.nlm.nih.gov/) and Ensembl ID (http://www.ensembl.org/) as well as the number of amino acids of the protein

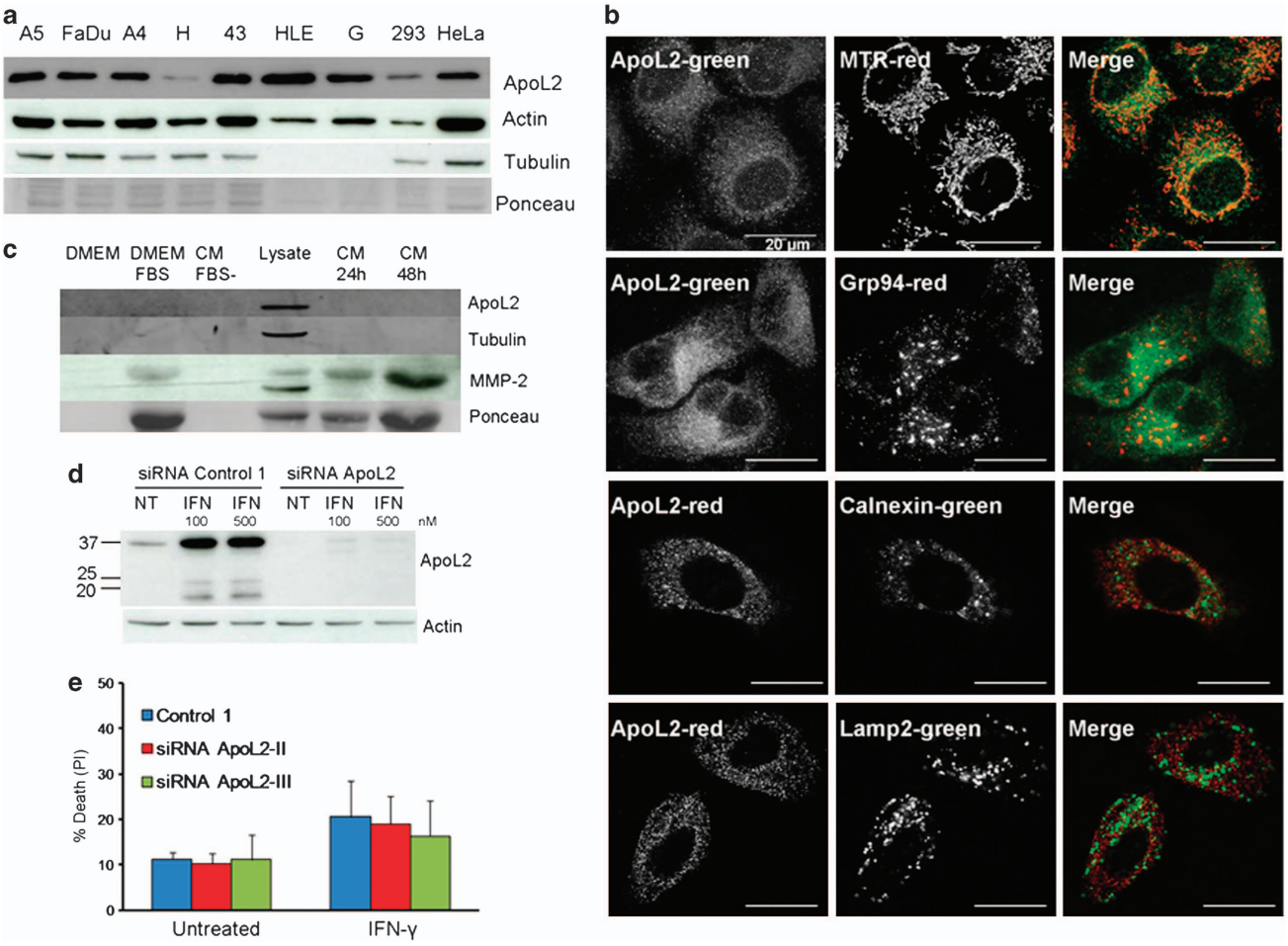

Figure 2 Cytosolic ApoL2 is widely expressed in different cell lines and induced by interferon-gamma. (**a**) ApoL2 expression was tested in different cell lines by western blot: A549 (A5), FaDu, A-431 (A4), HCT116 (H), 435P (43), HLE, HepG2 (G), HEK293 (293) and HeLa cells. (**b**) Intracellular localization of ApoL2. HeLa cells were stained with MitoTracker red (MTR) as mitochondrial marker. Antibodies against Grp94 and Calnexin were used as endoplasmic reticulum markers. Lysosomal localization was studied using Lamp-2 antibody. Scale bars of 20 μm are shown. (**c**) ApoL2 is not secreted. Western blot of trichloroacetic acid (TCA)-concentrated medium or cell lysate is shown. DMEM and DMEM complemented with FBS were used as controls. CM FBS $-$: conditioned medium of HeLa cells grown for 48 h in DMEM without FBS. Lysate: cell lysate of HeLa cells grown in FBS containing medium for 48 h. CM: conditioned medium of HeLa cells grown in FBS containing medium for indicated times. Antibodies against ApoL2, tubulin, actin and the secreted protein metalloproteinase-2 (MMP-2) were used for immunoblotting. (**d**) HeLa cells were transfected with siRNA ApoL2-II, treated with interferon-gamma (IFN) at 100 or 500 nM for 24 h and collected for western blot. NT means non treated. (**e**) HeLa cells were transfected with siRNA control 1 or siRNA against ApoL2 and treated with IFN-γ 100 nM for 72 h. Cell death was measured by PI incorporation at the flow cytometer. Figure shows average and S.E.M. of three independent experiments

reach statistical significance ($n=3$). Bcl-2 was employed as a control (expression checked in Supplementary Figure 3) and it protected from Noxa and Bmf.

Next we analyzed whether ApoL2 would regulate cell death induced by a variety of stimuli, either by behaving as an antiapoptotic protein as described[14] or as a proapoptotic

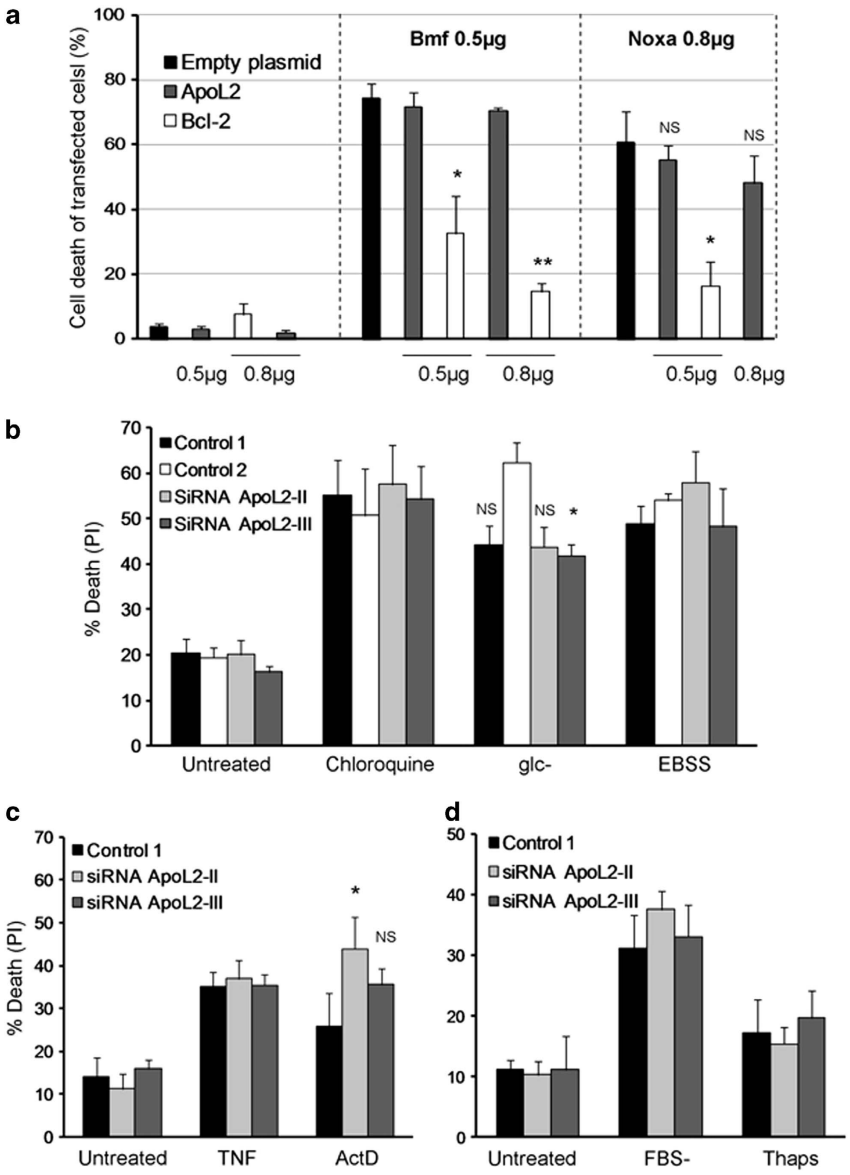

Figure 3 ApoL2 does not regulate cell death of HeLa cells. (**a**) Plasmids encoding two different BH3-only proteins (0.5 μg of Bmf and 0.8 μg of Noxa plasmids) were cotransfected with ApoL2 or Bcl-2 and analyzed by microscopy. GFP (0.3 μg) was used as transfection marker. ApoL2 and Bcl-2 plasmids were used at amounts shown. Empty plasmid was used to normalize the amount of transfected DNA. Dead green cells were scored by shrunk morphology and counted from images using fluorescence microscopy. Figure shows average and S.E.M. of three experiments. For statistical analysis, each ApoL2 or Bcl-2 overexpressing condition has been compared with the empty plasmid condition transfected with the same BH3-only protein. NS, nonsignificant. (**b**, **c**, **d**). HeLa cells were transfected with different control siRNAs or siRNA against ApoL2 and then treated with chloroquine, deprived of glucose (glc $-$), incubated in starvation buffer (EBSS) or treated with tumor necrosis factor (TNF) or actinomycin D (ActD) for 24 h (**b**, **c**), or deprived of serum (FBS $-$) or treated with thapsigargin (Thaps) for 72 h (**d**). Cell death was measured by PI incorporation by flow cytometry. Figure shows average and S.E.M. of three (**d**) or five experiments (**b**, **c**). Asterisks or NS (nonsignificant) denote significance *versus* Control 2 (**b**) or Control 1 (**c**)

BH3-only protein like ApoL1 and ApoL6. We knocked down ApoL2 using different siRNA sequences and treated HeLa cells with the endoplasmic reticulum stressor thapsigargin, the DNA damaging agent actinomycin D, the lysosomal inhibitor chloroquine, or starvation of serum, glucose or serum/amino acid/vitamins (culture in EBSS buffer) (Figures 3b–d). We only observed a minor difference in cell death induced by actinomycin D that was significant when cells were depleted of ApoL2 using one siRNA oligo but not the second one. ApoL2 has been shown to be induced by TNF.[6] We did not observe induction of ApoL2 upon TNF treatment in HeLa or 293T cells (Supplementary Figure 4). In addition, we treated HeLa cells with TNF in the presence of cycloheximide to induce cell death, and we did not observe any difference when ApoL2 was silenced (Figure 3c).

ApoL2 interacts weakly with Bcl-2 but it does not regulate autophagy. We could not detect a role of ApoL2 in cell death. However, not all BH3-only proteins described to date regulate cell death. Some proteins like Beclin-1 regulate autophagy through its interaction with Bcl-2 family proteins. ApoL6, which induces cell death and inhibits autophagy, has

been shown to bind Bcl-xL.[17] We thus tested whether endogenous ApoL2 interacted with other BH3-containing proteins. We immunoprecipitated ApoL2 and blotted for multidomain Bcl-2 family proteins. Bcl-2 was reproducibly immunoprecipitated with ApoL2 (Figure 4a). We were unable to immunoprecipitate endogenous Bcl-2 under the same conditions (not shown). For these reasons, to confirm these interactions in a different manner we overexpressed HA-tagged Bcl-2.[18] Under these conditions, we were unable to immunoprecipitate ApoL2 with anti-HA antibody (Figure 4b) or to detect HA upon immunoprecipitation of ApoL2, neither in HeLa nor in 293T cells (not shown). We next checked whether the weak interaction between ApoL2 and Bcl-2 (detected only using endogenous proteins) would alter the sensitivity of HeLa cells to the Bcl-2 and Bcl-xL inhibitor ABT-737. Downregulation of ApoL2 did not alter the amount of cell death induced by ABT-737 (Figure 5a).

One possibility is that ApoL2, by interacting with Bcl-2 or signaling lipids, would regulate cell proliferation. We tested this and could not observe any effects on cellular proliferation by downregulation of ApoL2 (Figure 5b). We next investigated whether ApoL2 could act like Beclin-1 or ApoL6 regulating autophagy.[17] We downregulated ApoL2 (Figures 6a and b) and measured basal autophagy (lipidation of LC3 and degradation of p62 in the presence or absence of protease inhibitors) and starvation-induced autophagy (same measurements after incubation in starvation buffer EBSS). Our results indicate that ApoL2 does not alter basal or starvation-induced autophagic flux as measured by levels of LC3-II (Figures 6a and c). We did observe a significant reduction of p62 levels after ApoL2 was downregulated, suggesting that this protein regulates basal autophagy (Figures 6a and d), but this was not accompanied by a difference in levels of LC3-II at these conditions (Figure 6c).

Altogether, our data indicate that ApoL2 is not a classical BH3-only protein, and its exact function in cell death by interferon treatment remains to be determined.

Discussion

BH3-only proteins do not share a high degree of homology between them, and it is possible that the BH3-domain arose either randomly during evolution or by a process of convergent evolution.[19] Moreover, the BH3-domain is not extremely well conserved even among Bcl-2 family proteins that share more domains than the BH3.[3] Many BH3-only proteins have not been identified by sequence, but on the basis of their interaction with Bcl-2 family proteins. Other members of this family have been found to be proapoptotic proteins and the putative BH3-motif was identified later. We have performed here a search based on a newly-generated protein composition profile that was shown to identify all known BH3-only proteins plus few additional candidates in the human genome.

Our screening identified the protein PXT1, which has a BH3-like domain. This protein has been described to induce cytochrome c release and apoptosis in HeLa cells in a manner dependent on its BH3 motif.[13] In addition, apolipoprotein L2 (ApoL2) caught our attention due to the recent description of ApoL2 homologs as BH3-only proteins. ApoL1, the founding member of the family, was identified as a component of a class of high density lipoproteins (HDL) in human blood.[20] In subsequent years, a number of homologous proteins have been described: the apolipoprotein L family comprises six members in humans and 8–14 members in rodents.[16,21] ApoL1 is the only member of the family expected to be secreted, and when internalized by trypanosomes it generates pores in their lysosomal membrane.[8] ApoL1 and ApoL6 also kill mammalian cells when overexpressed, and it has been proposed that all members of the family could share this ability with these two proteins.[9] Induction of cell death by ApoL1 and ApoL6 was prevented when their BH3 motif was deleted.[5,7] Both proteins bind lipids;[5,7] interestingly, ApoL1 binds cardiolipin which is a lipid required for permeabilization of liposomes by Bcl-2 family members.[22] ApoL6 binds Bcl-xL

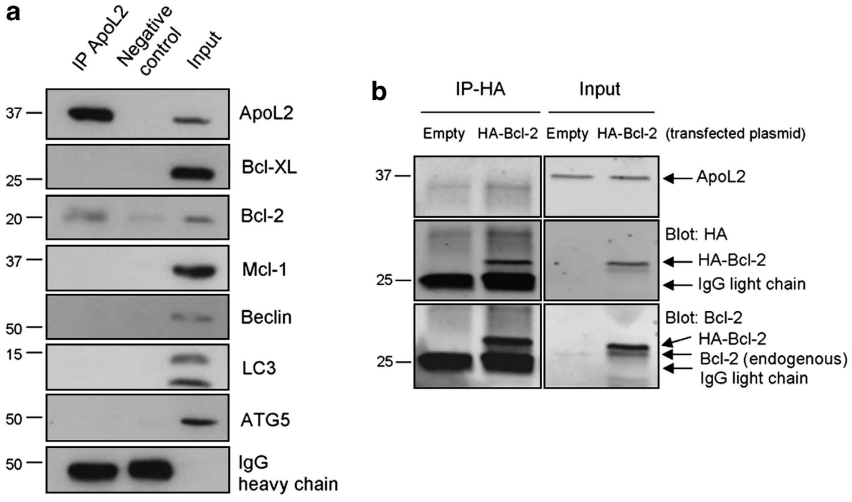

Figure 4 Immunoprecipitation of ApoL2 in HeLa cells. (**a**) Endogenous ApoL2 was immunoprecipitated (IP) and the presence of the indicated proteins was assayed by western blot. Blots from a single experiment representative of three independent experiments are shown. (**b**) HeLa cells were transfected with HA-Bcl-2 or empty vector. Anti-HA was used for immunoprecipitation and the presence of ApoL2, Bcl-2 and HA was assayed by western blot. Panel shown is representative of three independent experiments. Left and right panels were cropped from the same films

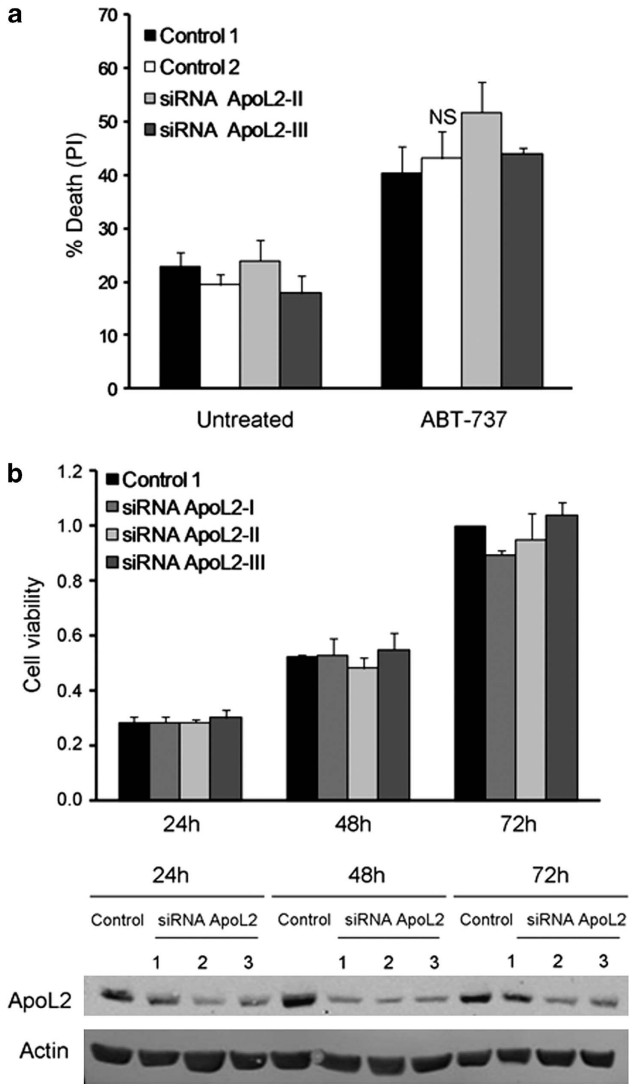

Figure 5 ApoL2 does not regulate cell proliferation or sensitivity to ABT-737. (**a**) HeLa cells were transfected with control siRNA or siRNA targeting ApoL2 and then they were treated with the BH3 mimetic ABT-737 at 30 μM for 24 h. Cell death was measured by PI incorporation and flow cytometry. Panel shows average and S.E.M. of five independent experiments. (**b**) HeLa cells were transfected with control 1 siRNA or siRNAs against ApoL2 and growth analysis was performed at indicated time points by crystal violet coloration. The lower panel shows western blot analysis of ApoL2 silencing over time

and it regulates autophagy.[17] So indeed, many similarities exist between some members of the apolipoprotein L family and 'classic' Bcl-2 family proteins.

ApoL2 has been shown to be antiapoptotic in primary cells treated with interferon-gamma.[14] Recently, ApoL2 has been identified as a protein that translocates to mitochondria in cells infected with H3N2 swine influenza virus.[23] These two facts, together with the description of other proteins of the family as BH3-only proteins has led to propose that ApoL2 has a role in apoptosis, which we have not been able to confirm. It is possible that the aspartic residue in position 10 of the motif (Figure 1) is essential for their proapoptotic function. The function of other Bcl-2 family members with a glutamic acid in that position, Bcl-Rambo (Bcl2L13) and Bcl-G (Bcl2L14), is still not fully defined, but their main function may be unrelated to cell death.[24,25]

We have detected a weak interaction between Bcl-2 and ApoL2. However, this did not alter apoptosis induced by many stimuli or starvation-induced autophagy. We did observe a basal regulation of p62, an autophagic protein, which could suggest that this protein regulates autophagy under certain conditions due to its interaction with Bcl-2. On the other hand, Bcl-2 regulates multiple metabolic pathways, Ca^{2+} stores in the endoplasmic reticulum, mitochondrial morphology and DNA repair.[26,27] We have not explored here the possibility that ApoL2 regulates these functions of Bcl-2. Nonetheless, it is also possible that the ApoL2 has a cell-type or stimulus-dependent role on cell death that according to our data is not general or ubiquitous.

Materials and Methods

Building the HMM. Sequences of vertebrate proteins annotated with the BH3-domain in Uniprot and the literature as of November 2008 (Bcl-2, Bcl-XL, Bcl-w, Mcl-1, Bcl-Rambo, Bcl-G, Bax, Bak, Bok, Bim, Bid, Bad, Bmf, Noxa, Hrk, Puma, Bik, Blk, Mule, Spike, Nix, BNIP3, Map-1, Cul7, Beclin-1, p53, ApoL6, ApoL1 and AVEN) were aligned with MAFFT.[28] A 15-residue long region from the alignment containing the annotated BH3 domains was selected using trimAl 1.3,[29] and a HMM model was built for the region using HMMER v1.8.5.[30] HMMER was used to search in the entire human proteome, as retrieved from Ensembl database version 50.[31] To detect the domain in putative unpredicted proteins we ran Exonerate[32] using that profile over the genome sequence. The results were compared with similar searches using the profiles available at PFAM (which rendered only already-annotated proteins) and Prosite databases, as well as with regular expression searches with motifs described in the literature (Table 1).

Cell culture and treatments. HeLa cells from American Type Culture Collection and 293T were cultured in pyruvate-free high glucose Dulbecco's Modified Eagle's Medium (DMEM; Gibco Life Technologies, Waltham, MA, USA) supplemented with 10% fetal bovine serum (FBS; Invitrogen, Carlsbad, CA, USA), 200 mg/ml of penicillin, 100 μg/ml of streptomycin and glutamine 2 mM (hereafter referred to as PSQ). Cells were maintained at 37 °C and in a 5% CO_2 atmosphere. Cell maintenance is based on three splits per week using trypsin EDTA-Solution 0.05% (Invitrogen). HeLa cells were plated at a concentration of 150 000/ml in 6- or 12-well plates and treated 24 h later, when they reached the concentration of 500 000/ml. 293T cells were plated at a concentration of 1×10^6/ml in 10 cm plates for transfections.

Before glucose-deprivation or FBS-deprivation treatments, cells were washed twice with FBS-free, pyruvate-free DMEM medium without glucose (Gibco Life Technologies) or high-glucose, FBS-free DMEM, respectively. Glucose-deprivation treatment is performed in PSQ-containing, glucose-free DMEM medium without glucose supplemented with 10% dialyzed FBS. FBS-deprivation treatment was performed in PSQ-containing high-glucose DMEM. For induction of cell death by starvation in Earle's Balanced Salt Solution (EBSS, Gibco Life Technologies), cells were washed twice with EBSS before treating with EBSS supplemented with Hepes 25 mM.

ABT-737 (Selleck Chemicals, Houston, TX, USA) is used at 30 μM, chloroquine, thapsigargin and actinomycin D (Sigma-Aldrich, St. Louis, MO, USA) at 100μM, 100 μg/ml and 50 nM, respectively, interferon-gamma (Novus Bionova, Madrid, Spain) at 100 ng/ml. TNF-α (Peprotech, Le-Perray-en-Yvelines, France, 10 ng/ml) is added in combination with 10 μM cycloheximide (Sigma-Aldrich) to induce cell death.

For autophagy induction, cells were incubated in home-made EBSS (potassium chloride 400 mg/ml, sodium bicarbonate 2.2 g/ml, sodium chloride 6.8 g/ml, NaH2PO4-H2O 140 mg/ml, D-Glucose 1 g/ml) supplemented with 25 mM Hepes. EBSS-Hepes treatment is performed after washing the cells twice with EBSS.

Autophagy flux was blocked by adding the protease inhibitors pepstatin A and E64d (Sigma, St. Louis, MO, USA, 10 μM each) simultaneously with the treatments.

Cell viability. For analysis of viability, cells were harvested by combining floating cells in the medium and adherent cells detached by trypsinization, and subjected to FACS analysis to detect incorporation of propidium iodide 1 μg/ml

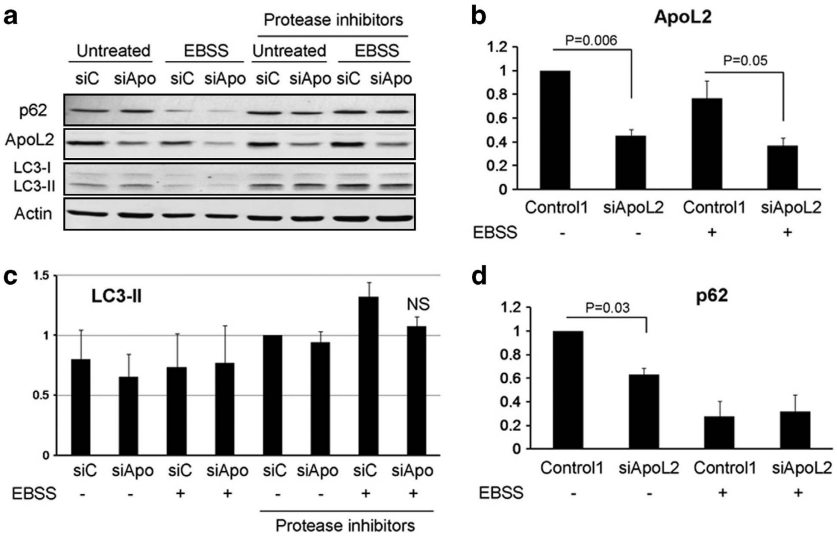

Figure 6 ApoL2 does not regulate autophagy. HeLa cells were transfected with siRNA Control 1 (labeled as siC) or siRNA against ApoL2-II (labeled as siApo) for 48 h and then the medium was changed or they were incubated with EBSS for 6 h to induce autophagy. The protease inhibitors pepstatin and E64D (10 μM each) were used to block autophagic flux. A representative western blot is shown in **a**. ApoL2 levels were quantified and are shown in **b**: data were weighted to ponceau or actin and then normalized against Control 1-transfected untreated cells. (**c**) Quantification of relative LC3-II levels: data were weighted to ponceau or actin and then normalized against Control 1-transfected HeLa cells with protease inhibitors as control of basal autophagy. (**d**) Quantification of relative p62 levels: data were weighted to ponceau or actin and then normalized against Control 1-transfected untreated cells. Graphs show average and S.D. of three independent experiments

(10 min incubation in PBS) using Gallios Flow Cytometer Beckman Coulter. Data were analyzed using FlowJo software, version 7.6.4.

Cell viability and number was additionally measured by crystal violet coloration. After the indicated treatments, cells were covered with staining solution (0.2% crystal violet, 2% EtOH solution) and incubated for 20 min at room temperature. Cells were rinsed twice with PBS and once with water and let dry for 16 h. Crystal violet-stained cells were then resuspended in 10% SDS and absorbance was read at 595 nm in a BioTek (Winooski, VT, USA) PowerWave XS microplate spectrophotometer.

Western blotting. Cell pellets were resuspended in RIPA buffer (Thermo Scientific, Waltham, MA, USA) or lysis buffer (0.06 M Tris, 2% SDS) containing protease inhibition cocktail (Roche, Basel, Switzerland) and phosphatase inhibitors (PhosSTOP, Roche) and they were then sonicated.

For trichloroacetic acid (TCA) precipitation, the acid (Merck, Darmstadt, Germany) was added to the sample at a final concentration of 13%, mixed thoroughly and incubated overnight at 4 °C under rotation. The mixture was centrifugated (16 000 $\times$ *g*, 15 min, 4 °C), and the supernatant was discarded. The pellet was resuspended in RIPA buffer.

Protein quantification was performed using Pierce BCA protein assay kit, following the manufacturer's instructions. 40 μg of protein were diluted in 10 μl of laemmli buffer 4 $\times$ (63 mM Tris-HCl, 10% glycerol, 2% SDS, 0.01% bromophenol blue and 5% 2-mercaptoethanol), and PBS was added until 40 μl of total volume. Lysates were boiled for 10 min at 96 °C and loaded in a 12% acrylamide gel. Mini-protean (Bio-Rad, Hercules, CA, USA) electrophoresis tank was used to perform the electrophoresis assay. Proteins were transferred to polyvinylidene fluoride (PVDF, Millipore, Darmstadt, Germany) or nitrocellulose membranes (Bio-Rad) through semi-dry transfer (1 h at 0.2 A/membrane). Transfer validation and loading charge control was checked by ponceau dye (Sigma). PVDF membranes were blocked with 5% nonfat dry milk in Tween Tris-buffered saline (TTBS) and processed for immunoluminiscence. Nitrocellulose membranes were blocked with Odyssey Blocking Buffer (LI-COR Biosciences, Lincoln, NE, USA) and processed for immunofluorescence using Odyssey Fc Imaging system. Primary and secondary antibodies were incubated for 1 h at room temperature or overnight at 4°C, in 5% milk TTBS. Three 10-min TTBS washes in the shaker were performed before developing by enhanced chemiluminescence (ECL; Pierce, Waltham, MA, USA) or scanning the membrane using Odyssey Imaging System. Quantification of band intensity was performed with Fiji/Image J software 1.47b.

Primary antibodies used for western blotting were: anti-actin (ICN clone 4), polyclonal anti-ApoL2 (Sigma, HPA001078), anti-tubulin (Sigma, Clone TUB 2.1). polyclonal antibody against p62 (Progen, Heidelberg, Germany), polyclonal anti-LC3 (Abcam, Cambridge, UK), anti-HA (Sigma, clone HA-7), anti-Bcl-xL (Cell Signaling, Beverly, MA, USA, 54H6), anti-Bcl-2 (Santa Cruz, Dallas, TX, USA, 100), polyclonal anti-Mcl-1 (Santa Cruz, sc-819), polyclonal anti-Atg5 (CosmoBio, Tokyo, Japan), anti-beclin-1 (BD Biosciences, Franklin Lakes, NJ, USA, 20/Beclin). HRP secondary antibodies were: antimouse and anti-rabbit (Zymax, Bideford, UK) or anti-guinea pig (Abcam). IRDye secondary anti-bodies against mouse or rabbit (IRDye 800CW donkey anti-rabbit IgG1 1/15.000 or IRDye 680LT anti-mouse IgG 1/20 000) were from LI-COR Biosciences.

Plasmids and transient transfection. ApoL2 cDNA (NM_030882.2) was purchased from Origene and subcloned into ampicillin resistant pcDNA3.1 plasmid using EcoR1 and BamH1 restriction enzymes. Invitrogen PureLink kit was used to extract the plasmid from competent bacteria (Promega, Fitchburg, WI, USA).

For death experiments, HeLa cells were transfected in six-well plates, using 4 μl of Genejuice (Novagen, Darmstadt, Germany) and 2 μg of total DNA. To normalize until 2 μg, we completed with the empty plasmid pcDNA 3.1. pcDNA 3.1-Bcl-2 plasmid was generously provided by Dr. Jean-Ehrland Ricci (Nice, France). HA-Noxa and pcDNA 3.1-Bmf were provided by Professor Seamus Martin (Dublin, Ireland). pcDNA 3.1-HA-Bcl-2 and pcDNA 3.1-HA-Bcl-xL plasmids from Dr. Douglas Green's laboratory (Memphis, TN, USA) were used in the immunoprecipitation assay. Cell death was analyzed by counting GFP positive dead cells against total GFP positive cells using an Olympus IX70 inverted microscope. For immunoprecipitation, HeLa cells were transfected in 10 cm dishes, using 3 μg of polyethylenimine linear (PEI; Polyscience Europe, Heidelberg, Germany) per μg of DNA. Cotransfection was performed using 10 μg of ApoL2 and 10 μg of HA-Bcl-xL or HA-Bcl-2 plasmid.

siRNA transfection. Cells were transfected at a density of 300 000/ml using 1.5 μl of DharmaFECT 1 (Dharmacon, Lafayette, CO, USA) per milliliter of total volume and following manufacturer's instructions. siRNA concentration was 100 nM. After 24 h, medium was replaced with growth medium. Control sequences were: 5′-GUAAGACACGACUUAUCGC[dT][dT] ('control 1') and an ON-TARGET plus siRNA pool of 4 oligos against mouse RIPK (Dharmacon; 'control 2'). Three different siRNA sequences were used against ApoL2: ApoL2-I (GCGGCAC CAAUGUAGCAAA[dT][dT]), ApoL2-II (CAGUGUGGUAGAACUAGUA[dT][dT]) and ApoL2-III (CAAUGUUCUUACCUUAGUU[dT][dT]).

Immunofluorescence. Cells were cultured on glass coverslips pretreated with poly-L-Lysine (Sigma). After 24 h they were incubated for 15 min in culture medium at 37 °C and 5% CO_2 with MitoTracker red 200 nM (Invitrogen) before

fixing, or they were directly fixed with a fresh 4% solution of paraformaldehyde for 20 min. Cells were then incubated with blocking buffer: 0.05% Triton, 3% BSA in PBS for 1 h and kept overnight at 4 °C with primary antibodies diluted 1 : 200 in blocking buffer: Ab rabbit anti-ApoL2 (Sigma), mouse anti-Lamp-2 (BD pharmigen, Franklin Lakes, NJ, USA, CD107b, 555803), mouse anti-Calnexin (Santa Cruz, E-10, sc-46669), goat anti-GRP94 (Santa Cruz, C-19, sc-1794). Cells were incubated with secondary antibodies Alexa Fluor 568 red and 488 green (Life Technologies, Carlsbad, CA, USA) diluted 1 : 400 in blocking buffer for 1 h. Then they were mounted in Vectashield solution (Vector laboratories, Burlingame, CA, USA) on microscope slides and visualized on a Leica TCS SP5 Spectral Confocal microscope with a HCX PL APO lambda blue $\times$ 63 1.4 oil objective lens. Acquisition software was LEICA (Wetzlar, Germany) Application Suite Advanced Fluorescence (LAS AF) version 2.6.0.7266 and pictures were analyzed with Fiji/Image J software.

Immunoprecipitation. A total of 30 μl of Protein G Magnetic Beads (Millipore) were washed 3 $\times$ in immunoprecipitation buffer and then incubated in 1 ml of immunoprecipitation buffer with 1 μg of antibody for 4 h at 4 °C under rotation. 10×10^6 cells were lysed in 500 μl of immunoprecipitation buffer (20 mM Tris-HCl (pH7.5), 137 mM NaCl, 1% Triton X-100, 2 mM EDTA (pH 8)) containing complete protease inhibitor cocktail and incubated for 30 min in ice. A total of 1400 μg of cell extract were incubated overnight in 1 ml of immunoprecipitation buffer with the antibody-coupled beads. The next day, beads were washed five times with immunoprecipitation buffer and eluted with 60 μl of immunoprecipitation buffer containing 2% SDS. Then 20 μl of laemmli buffer 4 $\times$ were added, and samples were boiled for 10 min at 95 °C. Eluted proteins were split in two gels of SDS-polyacrylamide gel electrophoresis. Ten percent of the total protein subjected to immunoprecipitation was loaded as input and 30 μl of the remaining supernatant after immunoprecipitation was also loaded to confirm immunodepletion. A total of 1 μg of anti-HA and anti-ApoL2 described above were used for immunoprecipitation.

Statistics. Error bars in the figures represent the standard error of the mean (S.E.M.). Data were statistically analyzed to find significant differences using two-tailed, paired Student's *t*-test. Significant differences are marked in the figures with * ($P \leq 0.05$) or ** ($P \leq 0.0005$).

Conflict of Interest

The authors declare no conflict of interest.

Acknowledgements. We wish to thank Dorothée Walter, Silvia Ramírez-Peinado, Dídac Domínguez and Clara León-Annicchiarico for help with experiments and Jean-Ehrland Ricci, Seamus Martin, Giulio Donati, Albert Tauler, Oscar M Tirado, Fabien Llambi, Pat Fitzgerald and Doug Green for plasmids, reagents and/or advice. This work was supported by the Association for International Cancer Research (AICR), grant number 08-0621 and Fondo de Investigaciones Sanitarias of Spain, grant numbers PI10/00104 and PI13/00139.

1. Droin NM, Green DR. Role of Bcl-2 family members in immunity and disease. *Biochim Biophys Acta* 2004; **1644**: 179–188.
2. Frenzel A, Grespi F, Chmelewskij W, Villunger A. Bcl2 family proteins in carcinogenesis and the treatment of cancer. *Apoptosis* 2009; **14**: 584–596.
3. Lomonosova E, Chinnadurai G. BH3-only proteins in apoptosis and beyond: an overview. *Oncogene* 2008; **27**: S2–S19.
4. Youle RJ, Strasser A. The BCL-2 protein family: opposing activities that mediate cell death. *Nat Rev Mol Cell Biol* 2008; **9**: 47–59.
5. Wan G, Zhaorigetu S, Liu Z, Kaini R, Jiang Z, Hu CA. Apolipoprotein L1, a novel Bcl-2 homology domain 3-only lipid-binding protein, induces autophagic cell death. *J Biol Chem* 2008; **283**: 21540–21549.
6. Zhaorigetu S, Wan G, Kaini R, Jiang Z, Hu CA. ApoL1, a BH3-only lipid-binding protein, induces autophagic cell death. *Autophagy* 2008; **4**: 1079–1082.
7. Liu Z, Lu H, Jiang Z, Pastuszyn A, Hu CA. Apolipoprotein l6, a novel proapoptotic Bcl-2 homology 3-only protein, induces mitochondria-mediated apoptosis in cancer cells. *Mol Cancer Res* 2005; **3**: 21–31.
8. Perez-Morga D, Vanhollebeke B, Paturiaux-Hanocq F, Nolan DP, Lins L, Homble F *et al.* Apolipoprotein L-I promotes trypanosome lysis by forming pores in lysosomal membranes. *Science* 2005; **309**: 469–472.
9. Vanhollebeke B, Pays E. The function of apolipoproteins L. *Cell Mol Life Sci* 2006; **63**: 1937–1944.
10. Sigrist CJA, de Castro E, Cerutti L, Cuche BA, Hulo N, Bridge A *et al.* New and continuing developments at PROSITE. *Nucleic Acids Res* 2013; **41**: D344–D347.
11. Finn RD, Bateman A, Clements J, Coggill P, Eberhardt RY, Eddy SR *et al.* Pfam: the protein families database. *Nucleic Acids Res* 2014; **42**: D222–D230.
12. Coultas L, Pellegrini M, Visvader JE, Lindeman GJ, Chen L, Adams JM *et al.* Bfk: a novel weakly proapoptotic member of the Bcl-2 protein family with a BH3 and a BH2 region. *Cell Death Differ* 2003; **10**: 185–192.
13. Kaczmarek K, Studencka M, Meinhardt A, Wieczerzak K, Thoms S, Engel W *et al.* Overexpression of peroxisomal testis specific 1 protein induces germ cell apoptosis and leads to infertility in male mice. *Mol Biol Cell* 2011; **22**: 1766–1779.
14. Liao W, Goh FY, Betts RJ, Kemeny DM, Tam J, Bay BH *et al.* A novel anti-apoptotic role for apolipoprotein L2 in IFN-gamma-induced cytotoxicity in human bronchial epithelial cells. *J Cell Physiol* 2011; **226**: 397–406.
15. Ahn WS, Bae SM, Lee JM, Namkoong SE, Han S-J, Cho YL *et al.* Searching for pathogenic gene functions to cervical cancer. *Gynecol Oncol* 2004; **93**: 41–48.
16. Page NM, Butlin DJ, Lomthaisong K, Lowry PJ. The human apolipoprotein L gene cluster: identification, classification, and sites of distribution. *Genomics* 2001; **74**: 71–78.
17. Zhaorigetu S, Yang Z, Toma I, McCaffrey TA, Hu CA. Apolipoprotein L6, induced in atherosclerotic lesions, promotes apoptosis and blocks Beclin 1-dependent autophagy in atherosclerotic cells. *J Biol Chem* 2011; **286**: 27389–27398.
18. Llambi F, Moldoveanu T, Tait SW, Bouchier-Hayes L, Temirov J, McCormick LL *et al.* A unified model of mammalian BCL-2 protein family interactions at the mitochondria. *Mol Cell* 2011; **44**: 517–531.
19. Aouacheria A, Brunet F, Gouy M. Phylogenomics of life-or-death switches in multicellular animals: Bcl-2, BH3-only, and BNip families of apoptotic regulators. *Mol Biol Evol* 2005; **22**: 2395–2416.
20. Duchateau PN, Pullinger CR, Orellana RE, Kunitake ST, Naya-Vigne J, O'Connor PM *et al.* Apolipoprotein L, a new human high density lipoprotein apolipoprotein expressed by the pancreas. Identification, cloning, characterization, and plasma distribution of apolipoprotein L. *J Biol Chem* 1997; **272**: 25576–25582.
21. Monajemi H, Fontijn RD, Pannekoek H, Horrevoets AJ. The apolipoprotein L gene cluster has emerged recently in evolution and is expressed in human vascular tissue. *Genomics* 2002; **79**: 539–546.
22. Kuwana T, Mackey MR, Perkins G, Ellisman MH, Latterich M, Schneiter R *et al.* Bid, Bax, and lipids cooperate to form supramolecular openings in the outer mitochondrial membrane. *Cell* 2002; **111**: 331–342.
23. Wu X, Wang H, Bai L, Yu Y, Sun Z, Yan Y *et al.* Mitochondrial proteomic analysis of human host cells infected with H3N2 swine influenza virus. *J Proteomics* 2013; **91**: 136–150.
24. Tischner D, Villunger A. Bcl-G acquitted of murder! *Cell Death Dis* 2012; **3**: e405.
25. Giam M, Okamoto T, Mintern JD, Strasser A, Bouillet P. Bcl-2 family member Bcl-G is not a proapoptotic protein. *Cell Death Dis* 2012; **3**: e404.
26. Hetz C, Glimcher L. The daily job of night killers: alternative roles of the BCL-2 family in organelle physiology. *Trends Cell Biol* 2008; **18**: 38–44.
27. Laulier C, Lopez BS. The secret life of Bcl-2: apoptosis-independent inhibition of DNA repair by Bcl-2 family members. *Mutat Res* 2012; **751**: 247–257.
28. Russell DJ, Katoh K, Standley D. MAFFT: iterative refinement and additional methods. In: *Multiple Sequence Alignment Methods*. Humana Press: Suita, Japan, 2014, pp 131–146.
29. Capella-Gutiérrez S, Silla-Martínez JM, Gabaldón T. trimAl: a tool for automated alignment trimming in large-scale phylogenetic analyses. *Bioinformatics* 2009; **25**: 1972–1973.
30. Eddy SR. Accelerated profile HMM searches. *PLoS Comput Biol* 2011; **7**: e1002195.
31. Flicek P, Amode MR, Barrell D, Beal K, Billis K, Brent S *et al.* Ensembl 2014. *Nucleic Acids Res* 2014; **42**: D749–D755.
32. Slater GS, Birney E. Automated generation of heuristics for biological sequence comparison. *BMC Bioinformatics* 2005; **6**: 31.

Supplementary Information accompanies this paper on Cell Death and Disease website (http://www.nature.com/cddis)

Cell Biology:

Glucose-starved Cells Do Not Engage in Prosurvival Autophagy

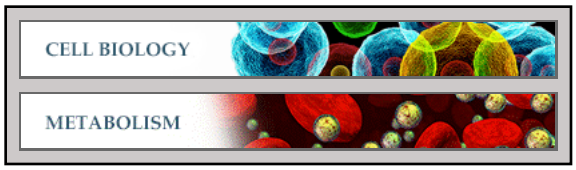

Silvia Ramírez-Peinado, Clara Lucía León-Annicchiarico, Javier Galindo-Moreno, Raffaella Iurlaro, Alfredo Caro-Maldonado, Jochen H. M. Prehn, Kevin M. Ryan and Cristina Muñoz-Pinedo

J. Biol. Chem. 2013, 288:30387-30398.
doi: 10.1074/jbc.M113.490581 originally published online September 6, 2013

THE JOURNAL OF BIOLOGICAL CHEMISTRY VOL. 288, NO. 42, pp. 30387–30398, October 18, 2013

Glucose-starved Cells Do Not Engage in Prosurvival Autophagy*

Received for publication, June 3, 2013, and in revised form, September 1, 2013 Published, JBC Papers in Press, September 6, 2013, DOI 10.1074/jbc.M113.490581

Silvia Ramírez-Peinado[‡], Clara Lucía León-Annicchiarico[‡], Javier Galindo-Moreno[‡], Raffaella Iurlaro[‡], Alfredo Caro-Maldonado[‡1], Jochen H. M. Prehn[§], Kevin M. Ryan[¶], and Cristina Muñoz-Pinedo[‡2]

From the [‡]Cell Death Regulation Group, IDIBELL (Bellvitge Biomedical Research Institute), L'Hospitalet de Llobregat, Barcelona, 08908 Spain, the [§]Department of Physiology and Medical Physics, Royal College of Surgeons in Ireland, 123 St. Stephen's Green, Dublin 2, Ireland, and [¶]Tumour Cell Death Laboratory, Cancer Research UK Beatson Institute, Glasgow G61 1BD, Scotland, United Kingdom

Background: Autophagy is a response to nutrient deprivation.
Results: Inhibition of autophagy does not sensitize cells to apoptotic or necrotic cell death induced by glucose starvation. Moreover, glucose deprivation inhibits autophagy.
Conclusion: 2-Deoxyglucose, but not glucose deprivation, induces autophagy.
Significance: Not all forms of starvation induce cytoprotective autophagy in mammalian cells.

In response to nutrient shortage or organelle damage, cells undergo macroautophagy. Starvation of glucose, an essential nutrient, is thought to promote autophagy in mammalian cells. We thus aimed to determine the role of autophagy in cell death induced by glucose deprivation. Glucose withdrawal induces cell death that can occur by apoptosis (in Bax, Bak-deficient mouse embryonic fibroblasts or HeLa cells) or by necrosis (in Rh4 rhabdomyosarcoma cells). Inhibition of autophagy by chemical or genetic means by using 3-methyladenine, chloroquine, a dominant negative form of ATG4B or silencing Beclin-1, Atg7, or p62 indicated that macroautophagy does not protect cells undergoing necrosis or apoptosis upon glucose deprivation. Moreover, glucose deprivation did not induce autophagic flux in any of the four cell lines analyzed, even though mTOR was inhibited. Indeed, glucose deprivation inhibited basal autophagic flux. In contrast, the glycolytic inhibitor 2-deoxyglucose induced prosurvival autophagy. Further analyses indicated that in the absence of glucose, autophagic flux induced by other stimuli is inhibited. These data suggest that the role of autophagy in response to nutrient starvation should be reconsidered.

Autophagy is an evolutionarily conserved cellular process activated upon starvation. In the absence of nutrients, cells engulf their own components in double membrane organelles called autophagosomes. These vesicles fuse to lysosomes, which promotes degradation of the content of the autophagosomes by digestive enzymes. This process produces new metabolites that can be used as new building blocks and as sources of energy (1, 2). For this reason, autophagy promotes cell survival under starvation (3).

Knockdown of genes essential for autophagy has been widely shown to enhance cell death in response to serum and amino acid starvation. However, it is presently unclear whether autophagy can help mammalian cells survive in the absence of glucose. Autophagy protects cancer cells from the glycolytic inhibitor 2-deoxyglucose (2-DG)[3] (4–6), which suggests that autophagy is a prosurvival response to glucose deprivation in mammalian cells. However, we and others (7, 8) have shown that glucose deprivation and 2-deoxyglucose do not exert cytotoxicity through the same pathways. Autophagy is a highly energy-consuming process, which involves organelle trafficking and maintenance of the ATP-dependent lysosomal pH, and it is unclear whether under conditions of low ATP autophagy would provide more energy. For this reason, we hypothesized that autophagy could actually be detrimental for cells deprived of glucose because it may end up consuming more ATP that it can produce by degrading intracellular components.

Nutrient starvation induces autophagy, at least in part, through activation of the AMP-activated protein kinase (AMPK)/mechanistic target of rapamycin (mTOR) energy sensing pathway. Activity of the autophagy-initiating complex containing ULK1 and ULK2 is controlled by mTOR and AMPK (9, 10), which are pathways regulated both by amino acids and glucose. This suggests that autophagy would be induced in a similar manner by glucose or amino acid starvation to provide nutrients for survival. Autophagy is protective for cells undergoing energetic stress such as hypoxic/hypoglycemic tumor cells, and the inhibition of autophagy was shown to promote necrotic cell death in apoptosis-deficient cells (11). We and others have previously shown that glucose deprivation kills cells either by apoptosis (caspase-dependent cell death) or necrosis (reviewed in Refs. 12 and 13). We thus aimed to study

* This work was supported by Fundació Marató TV3 Grant 111630/31 (to C. M.-P. and J. H. M. P.), Secretaria for Universities and Research (SUR) of the ECO of the Government of Catalonia fellowship (to R. I.), and Fondo de Investigaciones Sanitarias of Spain Grant PI10/00104 (to C. M.-P.).
[1] Present address: Dept. of Pharmacology and Cancer Biology, Duke University. Durham, NC.
[2] To whom correspondence should be addressed: IDIBELL, Hospital Duran i Reynals 3ª planta, Gran Via de L'Hospitalet 199, L'Hospitalet, 08908 Barcelona, Spain. Tel.: 34-93-260-7130; E-mail: cmunoz@idibell.cat.

[3] The abbreviations used are: 2-DG, 2-deoxyglucose; 3-MA, 3-methyladenine; EBSS, Earle's Balanced Salt Solution; MEF, mouse embryonic fibroblast; mTOR, mechanistic target of rapamycin; PI, propidium iodide; EGFP, enhanced GFP.

the role of autophagy in survival of cells that die by apoptosis and in cells that die by necrosis upon glucose deprivation. Surprisingly, we observed that in contrast to the current view, autophagy does not protect cells from glucose deprivation. Moreover, glucose deprivation did not induce autophagic flux.

EXPERIMENTAL PROCEDURES

Cell Culture and Treatments—The alveolar rhabdomyosarcoma cell line Rh4, Bax/Bak-deficient MEFs immortalized with SV-40 (14), HEK293 cells, and HeLa cells (American Type Culture Collection) were maintained in high-glucose (25 mM), pyruvate-free DMEM (Invitrogen) supplemented with 2 mM L-glutamine, 200 mg/ml penicillin, 100 mg/ml streptomycin sulfate, and 10% FBS (Invitrogen).

For treatments, Rh4 cells were plated at a concentration of 200,000/ml and treated in fresh medium 24 h later at 70–80% confluence (600,000/ml). HeLa and MEF cells were plated at a concentration of 150,000/ml and treated 24 h later, when they reached the concentration of 500,000/ml (1×10^6/ml HEK293).

Glucose deprivation was performed by rinsing the cells twice with glucose-free DMEM (Invitrogen/Invitrogen) and incubating them in glucose-free medium with freshly added 2 mM glutamine and antibiotics, plus 10% FBS dialyzed against PBS. Control cells were incubated in the same medium plus 25 mM glucose. Q-VD-OPH (SM Biochemicals LLC) as caspase inhibitor was used at 20 μM. 10 mM 2-deoxyglucose (Sigma) was added in regular culture medium. 10 mM metformin (1-1-dimethylbiguanide hydrochloride, Sigma) was used.

For induction of autophagy, cells were incubated in amino acid and serum-free, glucose-containing starvation buffers (Earle's starvation buffer (EBSS) or Hank's balanced salt solution, Invitrogen) or with 2 μM rapamycin (Calbiochem) or NVP-BEZ-235 (Selleck) in regular medium. EBSS was supplemented with 25 mM Hepes. Autophagy inhibitors as 20 nM bafilomycin A1 (Calbiochem, dissolved in dimethyl sulfoxide), chloroquine (Sigma), 3-methyladenine (Calbiochem, prepared in glucose-free medium or in starvation buffer), pepstatin A, and E-64d (Sigma-Aldrich) were added simultaneously with the treatments unless indicated. An equal amount of dimethyl sulfoxide was added to the controls for treatments with bafilomycin.

Measurement of Cell Death—For analysis of viability, cells were harvested by combining floating cells in the medium with adherent cells that were detached by trypsinization. Then they were subjected to FACS analysis to detect incorporation of 1 μg/ml propidium iodide (10-min incubation in PBS). For sub-G_1 analysis, cells were washed in PBS, fixed in 70% cold ethanol while vortexing, and incubated for 1–10 days at −20 °C. Cells were further washed, resuspended in PBS with 40 μg/ml propidium iodide and 100 μg/ml RNase A (Sigma), and incubated for 30 min at 37 °C before FACS analysis.

For analysis of cell death by incorporation of DAPI in the microscope (Fig. 3*C*), cells were stained with 0.5 μg/ml DAPI. 70 transfected (red) cells per condition were analyzed on an inverted Microscope Zeiss Axio Observer.Z1.

Western Blotting—Cells were trypsinized, washed with PBS, lysed by resuspending them in Pierce radioimmune precipitation assay (RIPA) buffer (Thermo Scientific: 25 mmol/liter Tris-HCl (pH 7.6), 150 mM NaCl, 1% Nonidet P-40, 1% sodium deoxycholate, 0.1% SDS) plus Complete antiprotease mixture (Roche Applied Science) and phosphatase inhibitor mixture tablets PhosSTOP (Roche Applied Science), and frozen. After sonication, protein concentration was measured with BCA protein assay reagent (Pierce). Equal amounts of protein were mixed with Laemmli loading buffer. After electrophoresis, protein was transferred to a polyvinylidene difluoride membrane (Millipore) or nitrocellulose blotting membranes (Bio-Rad). PVDF membranes were blocked with 5% nonfat dry milk in Tris-buffered saline/Tween 20 (0.1%). Secondary antibodies (1:5000) were HRP-conjugated (Sigma) and detected with ECL reagent (Pierce). Nitrocellulose membranes were blocked with Odyssey blocking buffer (LI-COR Biosciences), and secondary antibodies (IRDye 800CW donkey anti-rabbit IgG1 (1:15,000) or IRDye 680LT anti-mouse IgG (1:20,000) from LI-COR Biosciences) were detected by fluorescence with the Odyssey Fc Imaging system. Primary antibodies used for Western blot were as follows: actin (ICN clone C4), LC3 (Abcam, ab48394), p62 (Progen, GP 62-C; Enzo, BML-PW9860), phospho-S6 (Cell Signaling, 2211), S6 (Upstate, 05-781R), Beclin-1 (BD Pharmingen, 612112), phospho-acetyl-CoA carboxylase (Ser-79; Cell Signaling), acetyl-CoA carboxylase (Cell Signaling C83B10), phospho-4E-BP1 (Thr-37/46) (Cell Signaling, 9459), and 4E-BP1 (Cell Signaling, 9452).

Quantification of band intensity was performed with Fiji/ImageJ software 1.47b. Intensity of LC3 bands shown was calculated relative to the actin band from the same membrane, and each experiment was normalized to the control treated with protease inhibitors or bafilomycin.

Virus Production and Generation of Stable Cell Lines—Plasmids encoding GFP-LC3 (15), Hit 60 (MoMuLV gag-pol expression plasmid), and pCG (VSV-G envelope protein expression vector) were transfected into HEK293T cells. Cells were incubated in 10-cm dishes in antibiotic-free DMEM and incubated for 6 h using 2 μl of Lipofectamine 2000 (Invitrogen) and 10 μg of DNA. Viruses were collected after 24 h (first supernatant) and 48 h (second supernatant). Then, virus-containing medium was filtered (0.45-μm SFCA membrane filter; Millipore), and aliquots were frozen.

Target cells (Rh4 and HeLa) were plated at 50% confluence and incubated overnight. For infections, the culture medium was replaced by 1 ml of first supernatant supplemented with 8 μg/ml polybrene (Sigma) in a total volume of 5 ml of DMEM+10% FBS and then incubated at 37 °C for 6 h or overnight. The infection process was repeated using the second supernatant. 48 h later, infected cell populations were selected using 1 μg/ml Zeocin (InvivoGen).

DNA and RNA Transfections and Plasmids—For DNA transfections at autophagic flux experiments, cells were incubated in 12-well dishes, and the tandem mRFP-EGFP-LC3 plasmid (ptfLC3 (16)) was transfected in antibiotic-free DMEM and incubated overnight with 1 μl of polyethylenimine (Polysciences) and 1 μg of DNA; for Atg4B (C74A) plasmid, cells were transfected with 3 μl of polyethylenimine and 1 μg of DNA. pBabeBlast-Strawberry was generated by digestion of pmStrawberry-C1 (Clontech) with NheI and BamHI. The excised insert was then blunt-ended and cloned into SnaBI-

digested pBabeBlast. Orientation was determined by sequencing. mStrawberry-Atg4B-C74A was a kind gift of Tamotsu Yoshimori (Osaka University). This plasmid was digested with NheI and BamHI to isolate mStrawberry-Atg4B-C74A. This fragment was then blunt-ended and cloned into the SnaBI site of pBabe-Blast to generate pBabe-Blast-mStrawberry-Atg4B-C74A. Insert orientation was again determined by sequencing.

For transfections of siRNA, cells were incubated in antibiotic-free DMEM with 75 nmol/liter siRNA premixed with DharmaFECT 1 (Dharmacon) in 10-cm dishes. 18 h later, cells were trypsinized, plated, and 48 h after transfection were treated as indicated. Sense strain sequence for ATG7 was 5′-GUUUGUAGCCUCAAGUGUU-3′; Beclin-1 was 5′-CAGUUUGGCACAAUCAAUA-3′. As a control, a non-matching siRNA oligonucleotide (pBlue, 5′-GUAAGACACGACUUAUCGC-3′) was used. p62/SQSTM1 was down-regulated using Dharmacon (Lafayette, CO) On-Target SMARTpool (catalog no. M-047628-01); Dharmacon ON-TARGETplus non-targeting pool was used as a control.

Confocal Microscopy—Cells were cultured on glass coverslips pretreated with poly-L-lysine (Sigma), transfected with fluorescent constructs (if applicable), and treated with the indicated agents. Then, they were fixed with a fresh solution of paraformaldehyde for 15 min, washed with PBS twice, mounted in Vectashield (Vector Laboratories), and visualized at room temperature directly on a Leica TCS SP5 spectral confocal microscope with a HCX PL APO λ blue 63 × 1.4 oil objective lense. Acquisition software was LEICA application suite advanced fluorescence (version 2.6.0.7266). The projections of Z-stacks are shown. Vesicles (dots) from Z-stacks of whole-field images with multiple cells were analyzed with Fiji/ImageJ software followed by the Laplacian filter. Results are presented as mean rates and correlate with a measurement of the punctate area in a minimum of four independent images and 40 cells.

ATP Detection Assay—Cells were cultured in 96-well plates for 20 h before treatments. ATP levels were measured using ATPlite 1step Kit (PerkinElmer Life Science) following the manufacturer's instructions. Luminescence was measured at a microplate luminescence counter, Victor5 (PerkinElmer Life Science). A standard curve of ATPs was set up in the same microplate that was used for the experimental samples.

Statistics—Unless specified, a two-tailed, paired Student's *t* test was applied. N.S. indicates not significant; a single asterisk indicates $p < 0.05$, a double asterisk indicates $p < 0.01$, and a triple asterisk indicates $p < 0.001$.

RESULTS

Inhibition of Autophagy Does Not Sensitize Cells to Apoptosis or Necrosis Induced by Glucose Deprivation—We aimed to determine whether autophagy protects from apoptotic or necrotic cell death induced by glucose deprivation. For that aim, we subjected different cell lines to glucose deprivation in the presence of two different chemical inhibitors of autophagy. These inhibitors, although not selective, have been widely employed to analyze the role of autophagy in cell death. 3-Methyladenine (3-MA) is a PI3K inhibitor that can inhibit the phosphatidylinositol kinase VPS34 and thus prevent formation of autophagosomes. Chloroquine blocks lysosomal function and thus inhibits macroautophagy, chaperone-mediated autophagy, degradation of membrane proteins by endocytosis, and other lysosome-dependent processes. We subjected cells to glucose deprivation in the presence of 3-MA or chloroquine. We have shown previously that HeLa cells die in part by apoptosis (cell death prevented by caspase inhibitors) and in part by necrosis when subjected to glucose deprivation (17). In these cells, it was reported previously that autophagy is a protective mechanism against complete starvation (3). We observed that 3-MA did not sensitize HeLa cells to glucose deprivation, even though at doses commonly used to inhibit autophagy, 3-MA is toxic for these cells (Fig. 1, *A* and *B*).

We have previously shown that Bax/Bak-deficient MEFs die by caspase-8-mediated apoptosis when deprived of glucose (17). Strikingly, these cells are protected from glucose deprivation when incubated in the presence of 3-MA (Fig. 1, *C* and *D*). We analyzed a third cell type, the rhabdomyosarcoma cell line Rh4. These cells die in a necrotic manner in the absence of glucose as cell death cannot be rescued by caspase inhibitors (Fig. 1*E*). Although 3-MA on its own was also quite toxic to these cells, 3-MA prevented cell death of Rh4 cells by glucose deprivation (Fig. 1, *F–H*).

Chloroquine is widely employed to inhibit the last steps of autophagy because of its ability to neutralize the lysosomal pH. We treated the same cell lines with chloroquine in combination with starvation of glucose. The effects were in general quite different from those obtained with 3-MA. In Rh4 cells, which were markedly protected from cell death by 3-MA, chloroquine did not reduce cell death (Fig. 2*A*). Chloroquine mildly sensitized Bax/Bak-deficient MEFs (Fig. 2*B*) and HeLa cells (Fig. 2, *C* and *D*) to glucose deprivation. It should be noted that chloroquine is toxic to every cell line studied in a dose- and time-dependent manner (Fig. 2, *C* and *D*) (data not shown), and the sensitization observed is possibly due to an additive effect on signals involved in cell death.

Inactivation of Autophagy Sensitizes Cells to 2-Deoxyglucose and Starvation Buffer but Not to Glucose Deprivation—2-DG is a glucose analog that kills tumor cells by apoptosis and has been tested as an anti-tumor drug (12). Its toxic effects are generally attributed to interference with glycolysis and ATP depletion. However, we and others have shown that the effects of 2-deoxyglucose can be attributed to interference with *N*-glycosylation and endoplasmic reticulum stress rather than ATP depletion (7, 8). 2-DG has been shown to induce autophagy, and toxicity of 2-DG can be enhanced by treatment with 3-MA or with siRNA against Beclin-1 or Atg7 (4, 5). We verified that 3-MA but especially chloroquine sensitized Rh4 cells to 2-deoxyglucose (Fig. 2, *E* and *F*), corroborating previous results that suggest that the effects of 2-deoxyglucose and glucose deprivation are different.

Because these chemical inhibitors are quite unspecific (although we verified that they inhibit autophagy in our cells (data not shown and Fig. 2*G*), we employed siRNA to knock down genes involved in autophagy. We deliberately avoided the use of cells from mice deficient in autophagy genes because it has been shown that these cells up-regulate compensatory protein degradation pathways such as chaperone-mediated autophagy, which may protect from apoptosis and complicate

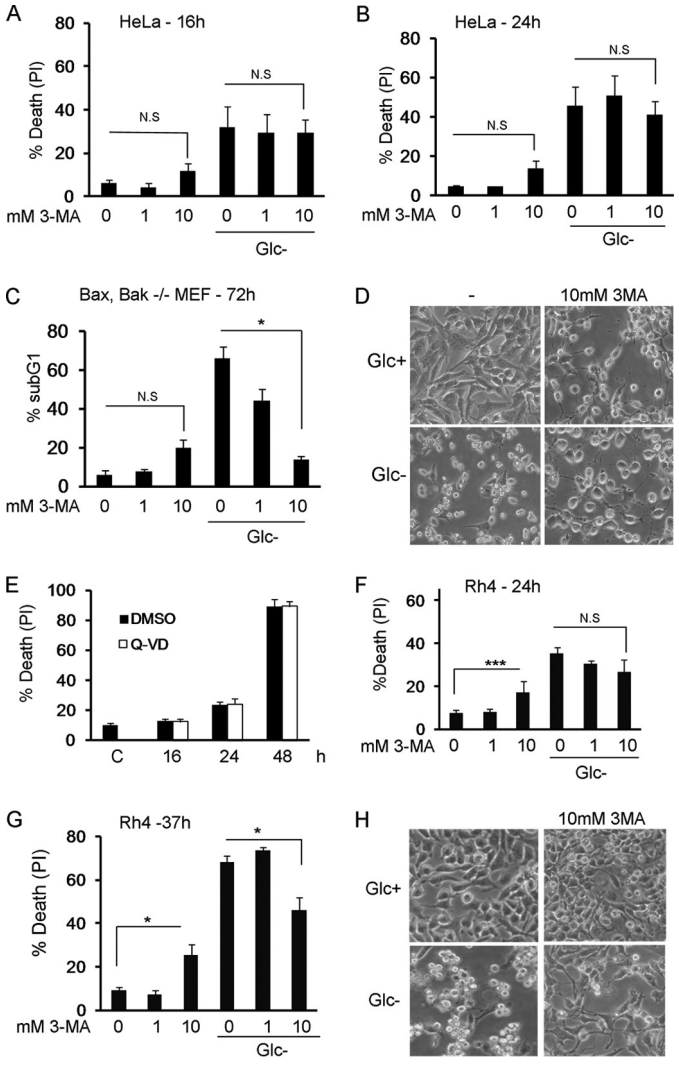

FIGURE 1. **3-Methyladenine inhibits apoptosis or necrosis induced by glucose deprivation.** *A* and *B*, HeLa cells were deprived of glucose in the absence or presence of 3-MA at indicated concentrations. Cell death was analyzed by propidium iodide incorporation at 16 (*A*) or 24 h (*B*). The figure shows the average and S.E. of three experiments. *C*, Bax/Bak$^{-/-}$ MEFs were subjected to glucose deprivation for the indicated times, in the absence or presence of 3-MA at indicated concentrations. Cells were collected for sub-G_1 analysis at the times shown. The figure shows the average and S.E. of three experiments. *D*, Bax/Bak$^{-/-}$ MEFs were treated with 10 mM 3-MA for 48 h in the presence or absence of glucose. Photographs show 80% of the field and were taken using a 20× objective. Note that 3-MA prevents cell shrinkage induced by glucose deprivation. *E*, Rh4 cells were grown in glucose-free medium in the presence of caspase inhibitors (Q-VD) or DMSO as vehicle control. Cells were collected at indicated times and subjected to propidium iodide (*PI*) uptake analysis. Data represent average and S.E. of three experiments. Untreated control cells (labeled *C*) were cells incubated in DMEM for 16 h. *F* and *G*, Rh4 cells were deprived of glucose in the absence or presence of 3-MA at indicated concentrations. Cell death was analyzed by propidium iodide incorporation at 24 h (*F*) or 37 h (*G*). The figure shows the average and S.E. of a minimum three experiments. *H*, Rh4 cells were treated with 10 mM 3-MA for 30 h in the presence or absence of glucose. Photographs showing 25% of the field were taken using a 20× objective. *N.S.*, not significant; *DMSO*, dimethyl sulfoxide.

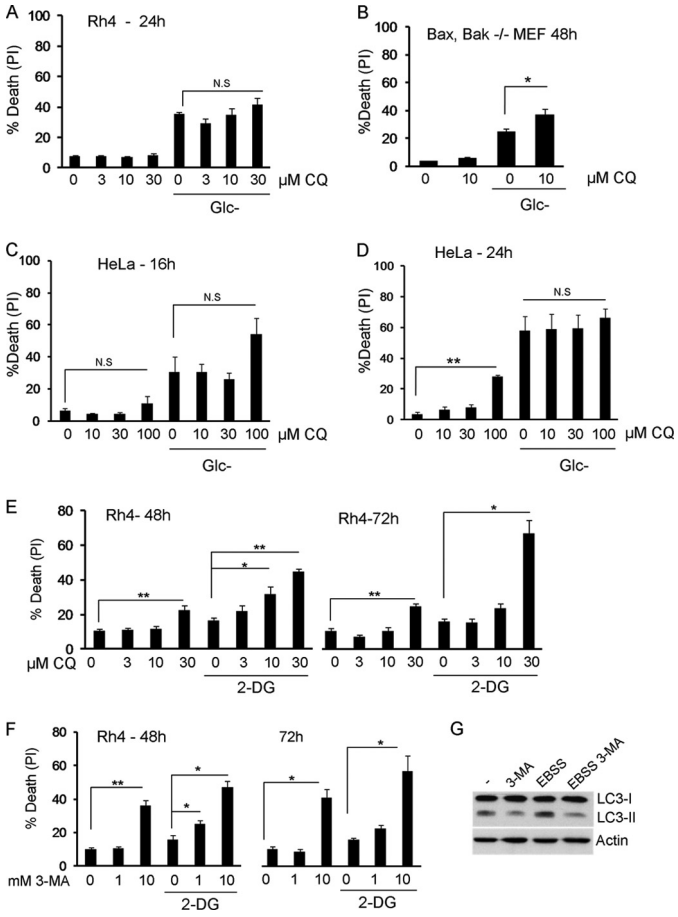

FIGURE 2. **Inhibition of lysosomal function with chloroquine promotes mild sensitization to glucose deprivation.** 3-MA and chloroquine sensitize to 2-deoxyglucose. *A*, Rh4 cells were deprived of glucose in the absence or presence of chloroquine (*CQ*) at indicated concentrations. Cell death was analyzed by propidium iodide incorporation after 24 h. The figure shows the average and S.E. of minimum four experiments. *B*, Bax/Bak$^{-/-}$ MEFs were subjected to glucose deprivation for the indicated times, in the absence or presence of 10 μM chloroquine. Cell death was analyzed by propidium iodide incorporation after 48 h. The figure shows the average and S.E. of three experiments. *C* and *D*, HeLa cells were deprived of glucose in the absence or presence of chloroquine at indicated concentrations. Cell death was analyzed by propidium iodide incorporation at indicated times. The average and S.E. of minimum three experiments are shown. *E*, Rh4 cells were treated with 2 mM 2-DG in the absence or presence of chloroquine at the indicated concentrations. Cell death was analyzed by propidium iodide incorporation after 48 and 72 h. The average and S.E. of six experiments are shown. *F*, Rh4 cells were treated with 2 mM 2-DG in the absence or presence of 3-MA at indicated concentrations. Cell death was analyzed by propidium iodide (*PI*) incorporation after 48 and 72 h. The figure shows the average and S.E. of a minimum four experiments. *G*, Rh4 cells were incubated with the protease inhibitors E64d and pepstatin A (20 μM each) for 6 h in regular medium (−) or EBSS, in the presence or absence of 3-MA (10 mM), and blotted for LC3 and actin. *N.S.*, not significant.

interpretation of results (18). We thus transiently silenced Beclin-1, a protein involved in nucleation of the phagophore. Down-regulation of Beclin-1 reduced basal and 2-DG-induced autophagy (Fig. 3*A*), and it clearly enhanced sensitivity of Rh4 cells to amino acid/serum starvation (incubation in EBSS) and to treatment with 2-deoxyglucose. However, only a minor sensitization to glucose deprivation was observed (Fig. 3*B*). We employed another genetic method that would inhibit autophagy even faster than the use of siRNA: we transfected Rh4 cells with a dominant-negative form of ATG4B that hampers the lipidation of LC3 paralogues (19). Transfected cells were highly sensitized to 2-DG and EBSS, and some basal cell death was observed at longer time points. However, these cells were not sensitized to glucose deprivation (Fig. 3*C*). We also transiently knocked down ATG7 in Bax/Bak-deficient MEFs, which die by apoptosis. The knockdown efficiency was modest (Fig. 3*D*) but sufficient to down-regulate basal and EBSS-in-

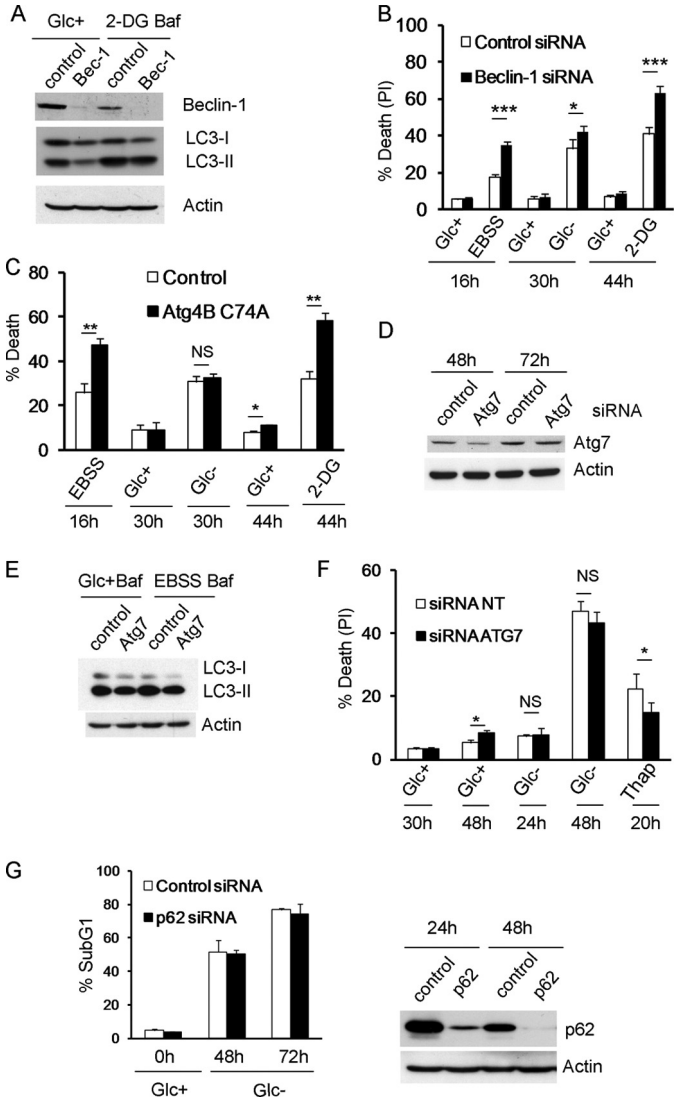

FIGURE 3. **Inhibition of autophagy sensitizes to 2-deoxyglucose and starvation buffer but not to glucose deprivation.** *A* and *B*, Rh4 cells were transfected with siRNA against Beclin-1 or control siRNA. *A*, 48 h after transfection, cells were treated with or without 2-DG for 48 h and bafilomycin (*Baf*) for the last 3 h of incubation. Protein was collected for Western blot. *B*, 48 h after transfection cells were treated with 2-DG, EBSS, or subjected to glucose deprivation for the indicated times. The average and S.E. of five experiments are shown. *C*, Rh4 cells were transfected with mStrawberry (Control) or mStrawberry-Atg4B (C74A) plasmids and incubated for 24 h. The cells were then cultured in EBSS, Glc+, Glc−, or 2-DG for the indicated times, and fluorescent (transfected) cells were scored as dead or alive with a low concentration of DAPI (see "Experimental Procedures"). *D–F*, Bax/Bak$^{-/-}$ MEFs were transfected with siRNA against ATG7 or control siRNA (*NT*, 5′-UAAGGCUAUGAGAGAUACtt). *D*, samples were collected for Western blot at times indicated. *E*, after 48 h of transfection, cells were cultured in regular culture medium or EBSS 95% + 5% medium and bafilomycin for 3 h and collected for Western blot. *F*, 48 h after transfection cells were cultured in Glc+, Glc−, or thapsigargin (1 μM) and collected for FACS analysis. The average and S.D. of three experiments are shown. *G*, Bax/Bak$^{-/-}$ MEFs were transfected with siRNA against p62 or control siRNA. 48 h later, they were deprived of glucose. Cell death was analyzed by sub-G_1 analysis. The average and S.D. of two experiments are shown. *Right panel*, cells were collected at times indicated after transfection for Western blot analysis. *PI*, propidium iodide; *NS*, not significant.

duced autophagy (Fig. 3*E*). Because these cells do not die with EBSS or 2-deoxyglucose for many days (data not shown), we employed thapsigargin as a control. This drug induces autophagy-dependent cell death in Bax/Bak-deficient MEFs (20). Indeed, knockdown of ATG7 reduced cell death induced by thapsigargin and promoted some cell death on its own at long time points, but it did not alter the response to glucose deprivation (Fig. 3*F*). We also silenced p62, a molecule involved in delivering cargo to autophagosomes. In the virtual absence of p62 cell death of Bax/Bak-deficient cells proceeded with identical kinetics (Fig. 3*G*).

Glucose Deprivation Does Not Induce Autophagic Flux—Inhibition of autophagy sensitized cells to 2-deoxyglucose but not to glucose deprivation. However, many studies had reported signs of autophagy in mammalian cells upon glucose deprivation (see Refs. 21–23). This prompted us to analyze whether glucose deprivation actually induced autophagic markers and, in particular, autophagic flux under our conditions of selective glucose deprivation. We generated HeLa and Rh4 cells stably expressing the autophagosomal marker LC3-GFP and starved them of glucose. Noticeable but modest puncta are observed in HeLa cells either growing under normal conditions or subjected to glucose deprivation (Fig. 4*A*). The fact that glucose deprivation does not induce an obvious translocation of LC3 could suggest that glucose deprivation does not induce autophagy; however, it is also possible that it is inducing autophagy, but autophagosomes are rapidly cleared by fusion with lysosomes. To distinguish between these two possibilities, we employed bafilomycin A1 to block lysosomal degradation of autophagosomal content. Bafilomycin A1 alone induced accumulation of LC3-GFP puncta, which indicates a high level of basal autophagy. However, incubation with bafilomycin A1 in the absence of glucose did not enhance the formation of the puncta (Fig. 4, *A* and *B*). Similar results were observed in Rh4 cells (Fig. 4, *C* and *D*). As controls, starvation buffers or the mTOR inhibitor rapamycin were used. Bafilomycin A clearly enhanced the formation of puncta triggered by these treatments (Fig. 4, *A–D*). We employed another method to analyze autophagic flux based on the lysosomal neutralization of GFP but not RFP (red fluorescent protein) fluorescence when these two molecules are fused to LC3. When LC3 is inside autophagolysosomes with acidic pH, only the red fluorescence is observed (16). We verified that incubation in starvation buffer EBSS or treatment with rapamycin induced autophagy in Rh4 cells, but glucose deprivation did not (Fig. 4*E*).

A different method to analyze autophagic flux is to measure the levels of p62 (an LC3-binding protein degraded by autophagy) and of lipidated (autophagosomal, LC3-II) LC3 by Western blot. We analyzed p62 and LC3-II levels after depriving cells of glucose. In HeLa cells, although levels of p62 are not reduced, LC3-II accumulates after treatment, which could indicate activation of autophagy (Fig. 5*A*). However, LC3-II accumulation may also mean autophagy is reduced compared with basal autophagy. When cells were incubated in regular culture medium in the presence or absence of inhibitors of the last stages of autophagy (the mixture of the protease inhibitors pepstatin A and E64D), LC3-II was accumulated at a much faster rate than in glucose-free medium. Moreover, the combination of glucose deprivation and protease inhibitors promotes similar or even lower accumulation (at long time points) than protease inhibitors alone. This indicates that although basal autophagy is high, glu-

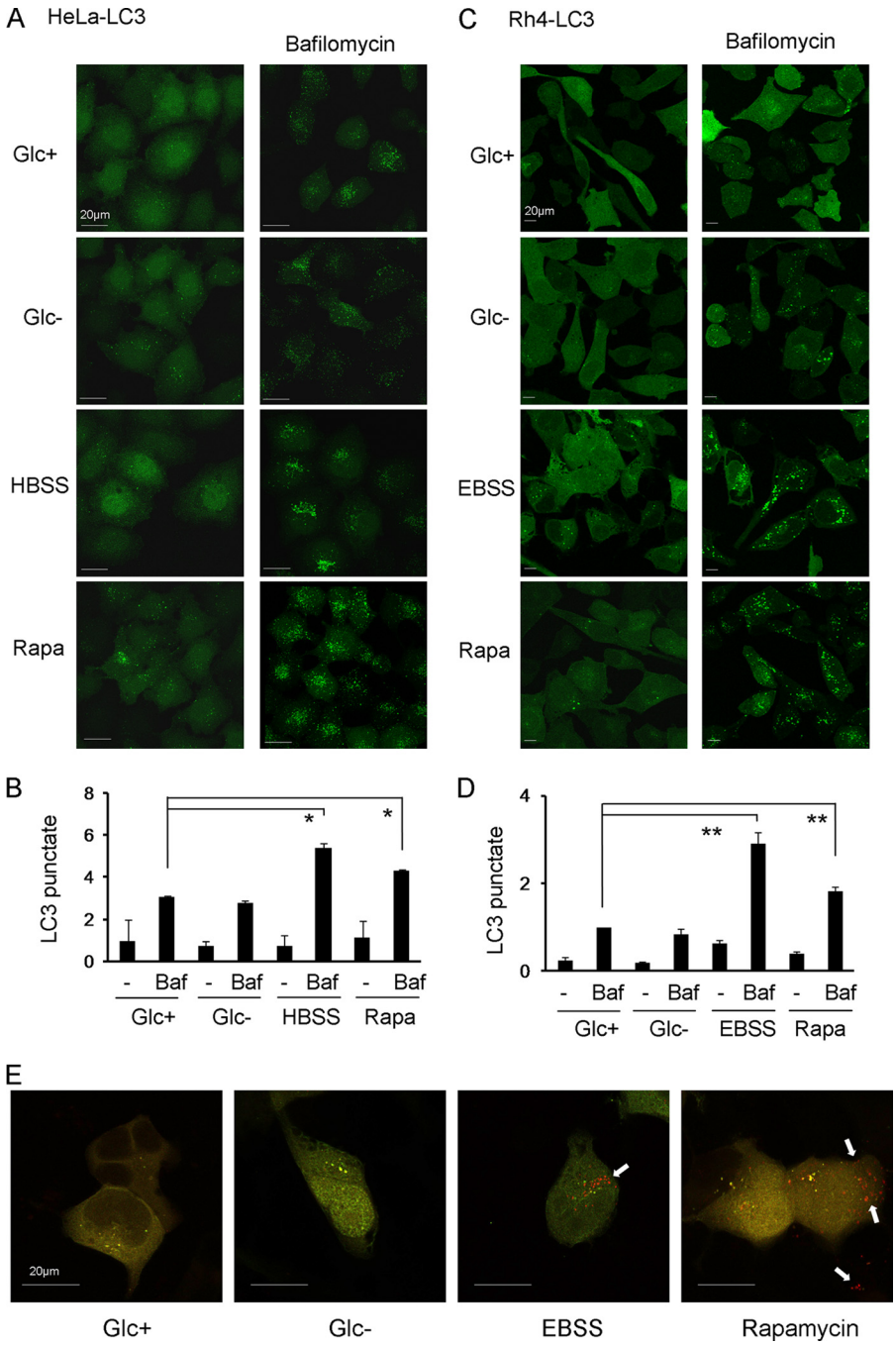

FIGURE 4. **Glucose deprivation does not induce autophagic flux.** *A–D*, HeLa (*A* and *B*) or Rh4 (*C* and *D*) stably transfected with GFP-LC3 (HeLa-LC3, Rh4-LC3) were treated with DMEM with glucose (Glc+), glucose deprivation (Glc−), amino acid deprivation (Hank's balanced salt solution/EBSS) or rapamycin (*Rapa*) for 6 h with or without bafilomycin (*Baf*) for the last 3 h. The expression pattern of GFP-LC3 was examined under a confocal microscope. Punctate LC3 in cells was measured as described under "Experimental Procedures." *B* and *D* show the mean + S.E. from two (HeLa, *B*) or four (Rh4, *D*) independent experiments. *E*, Rh4 were transfected with mRFP-GFP-LC3 plasmid and treated 24 h post-transfection for 15 h. Representative images from three independent experiments are shown. *Arrows* indicate *red* points (autophagolysosomes).

cose deprivation does not induce autophagy, and moreover, it seems to reduce it. In contrast, incubation in EBSS induced autophagy in HeLa (Fig. 5*A*) and in Bax/Bak-deficient cells (Fig. 5*B*). Intriguingly, glucose deprivation promotes the accumulation of p62 in these cells, suggesting that either glucose deprivation inhibits autophagic flux, whereas the rate of synthesis of p62 may remain the same, or that glucose regulates p62 levels independently of autophagy. LC3-II accumulated strongly upon depriving cells of glucose. However, the presence of bafilomycin A did not increase the levels of LC3-II. Altogether, these results suggest that both in HeLa and in Bax/Bak-deficient MEFs (that can be kept alone for almost 2 days without apparent toxicity (17)), glucose deprivation inhibits rather than induces autophagy. We then compared the effects of 2-deoxyglucose and glucose deprivation in Rh4 cells (Fig. 5, *C* and *D*). Glucose deprivation promoted a slow accumulation of LC3-II. However, bafilomycin A did not further increase this accumulation, suggesting that accumulation is due to inhibition. In

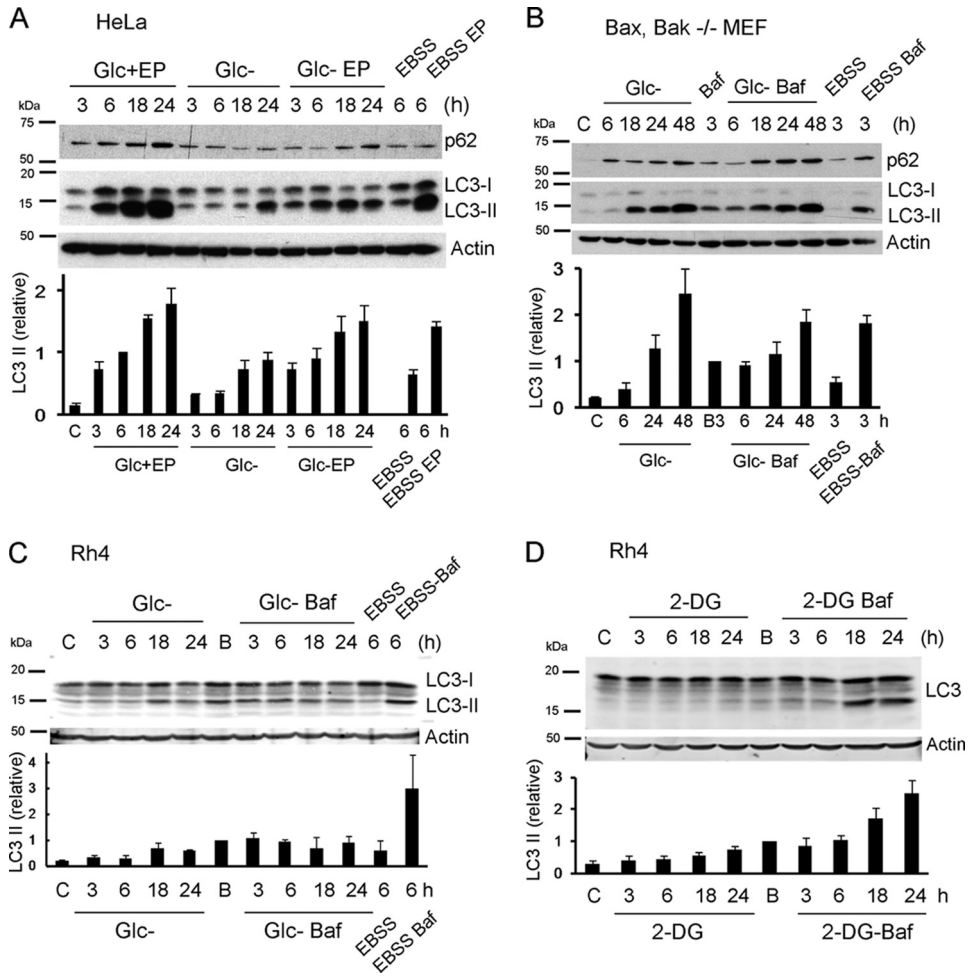

FIGURE 5. **Induction of autophagic flux by 2-deoxyglucose and starvation but not glucose deprivation.** *A*, HeLa cells were deprived of glucose or incubated in 95% EBSS+5% culture medium for the indicated times, in the presence or absence of E64d and pepstatin A (*EP*) (10 μM each). Proteins were resolved by SDS-PAGE and immunoblot. Bands immunoreactive with anti-LC3 antibody and with anti-p62 are shown. Untreated control cells (labeled *c*) were cells incubated in DMEM for 3 h. The *lower panel* shows quantification of relative LC3 II levels as described under "Experimental Procedures" (average and S.E. of minimum three independent experiments). *B*, Bax/Bak$^{-/-}$ MEFs were subjected to glucose deprivation or incubated in 95% EBSS+5% culture medium for the indicated times, in the absence or presence of 20 nM bafilomycin (*Baf*) for the last 3 h to avoid toxicity. Untreated control cells (labeled as *c*) were cells incubated in DMEM for 6 h in the presence (*B*) or absence (*C*) of bafilomycin for the last 3 h. Bands immunoreactive with anti-LC3 antibody and with anti-p62 are shown. The *lower panel* shows quantification of relative LC3 II levels as described under "Experimental Procedures" (average and S.E. of three independent experiments). *C*, Rh4 cells were subjected to glucose deprivation or incubated in 90% EBSS+10% culture DMEM for the indicated times, in the absence or presence of 20 nM bafilomycin for the last 3 h to avoid toxicity. Untreated control cells were cells incubated in DMEM for 3 h in the presence (*B*) or absence (*C*) of bafilomycin for the last 3 h. Proteins were resolved by SDS-PAGE and immunoblot. The *lower panel* shows quantification of relative LC3 II levels as described under "Experimental Procedures." Results are representative of three independent experiments; two for EBSS. *D*, Rh4 cells were treated with 2-DG for the indicated times, in the absence or presence of 20 nM bafilomycin for the last 3 h. Untreated control cells were cells incubated in DMEM for 3 h in the presence (*B*) or absence (*C*) of bafilomycin for the last 3 h. The *lower panel* shows quantification of relative LC3 II levels as described under "Experimental Procedures" (three independent experiments).

contrast, incubation of these cells in EBSS buffer or treatment with 2-deoxyglucose clearly induced autophagy.

Glucose Deprivation Engages Starvation Signals but It Inhibits Autophagy—Two possibilities are non-exclusive and compatible with the results described above. Glucose deprivation may not engage the same pro-autophagic signals triggered by amino acid starvation or by 2-DG. Or glucose may be required for completion of autophagy even if starvation signals occur. To examine these possibilities, we first analyzed whether the cell types that we used do not properly inactivate mTOR in response to glucose deprivation due, for instance, to constitutive hyperactivation of the mTOR pathway. We observed that in Rh4 cells (Fig. 6*A*) and in HeLa and Bax/Bak-deficient MEFs (data not shown), mTOR is inactivated upon glucose deprivation, as measured by S6 and 4EBP1 dephosphorylation. 2-Deoxyglucose, which induces autophagy in Rh4 cells, inhibited mTOR with similar kinetics (Fig. 6*A*). Inhibition of mTOR is usually considered sufficient to trigger autophagy, and mTOR inhibitors are *bona fide* autophagy inducers. However, it is possible that, if the signal to inhibit mTOR in the absence of glucose was not sufficiently strong, AMPK activation was also required to induce autophagy by phosphorylating ULK1, Vps34, and Beclin-1 (9, 10, 24). HeLa cells cannot activate AMPK upon energy stress because they lack the kinase LKB1, and we could not consistently detect phospho-AMPK or phosphorylation of its substrate phospho-acetyl-CoA carboxylase in Rh4 cells (data not shown). For this reason, we analyzed AMPK and autophagy activation in a cell line that has been used to

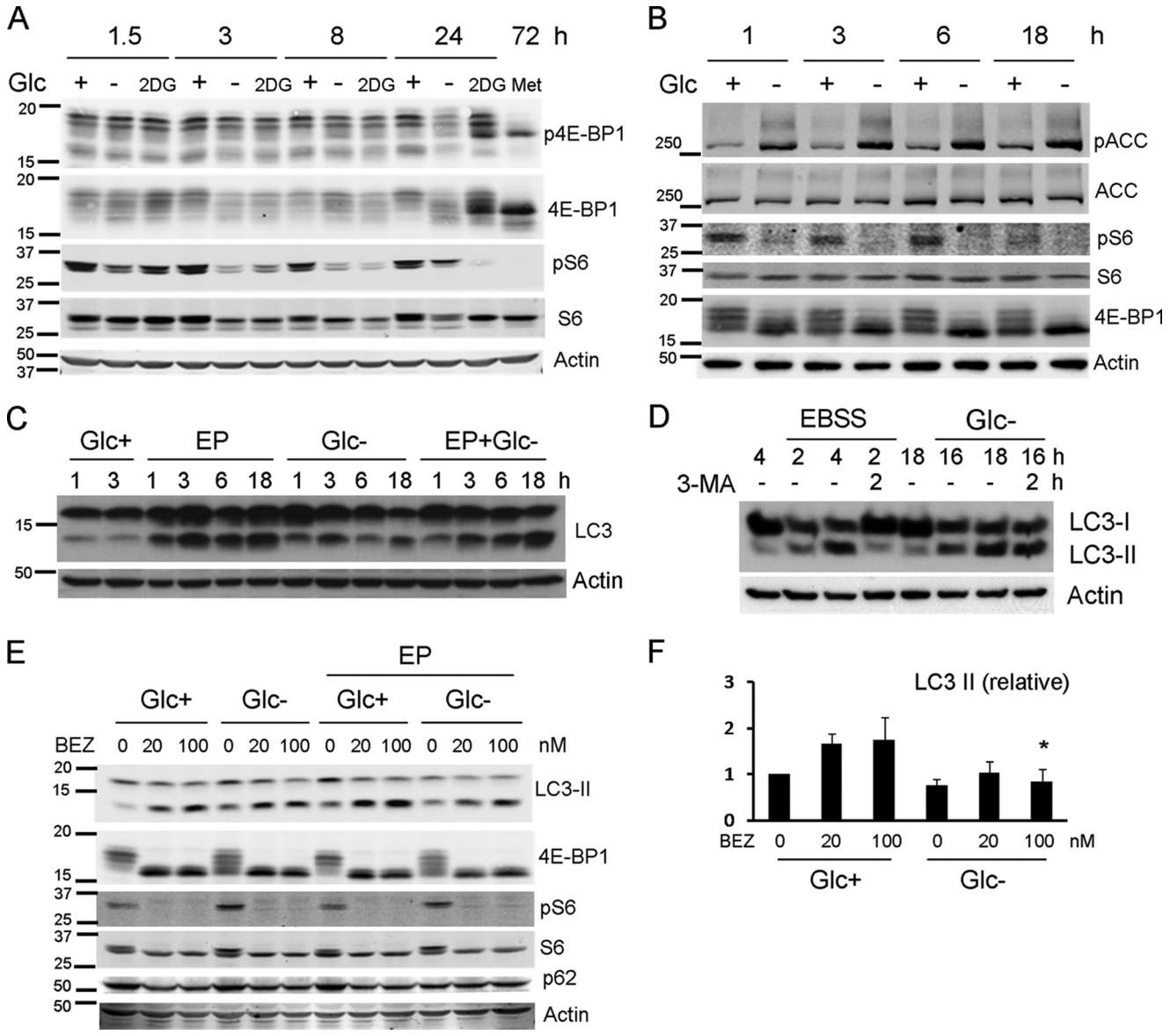

FIGURE 6. **Glucose deprivation engages starvation signals, but it inhibits autophagy.** *A*, Rh4 cells were treated with glucose-free medium, 2-DG, or metformin (*Met*) for the indicated times. Proteins were resolved by SDS-PAGE and immunoblot. Phospho-4E-BP1, 4E-BP1, phosphoS6, S6, and actin were detected using secondary infrared antibodies. *B*, HEK293 cells were incubated in glucose-free medium in the presence or absence of glucose. Proteins were resolved by SDS-PAGE and immunoblot. Phosphorylated and total acetyl-CoA carboxylase (*ACC*) and S6 proteins, 4E-BP1, and actin were detected using infrared antibodies. *C*, HEK293 cells were deprived of glucose for the times shown with or without E64d and pepstatin A (*EP*) at the concentration of 20 μM each, collected, and subjected to Western blot. *D*, Bax/Bak$^{-/-}$ MEFs were treated with or without glucose (Glc−) or EBSS for the indicated times (expressed in hours), followed by 2 h of treatment with 3-MA where indicated and collected for Western blot. *E*, Rh4 cells were incubated in glucose-free or glucose-rich medium for 15 h, in the presence or absence of E64d and pepstatin A at 20 μM each, and in the presence or absence of the mTOR inhibitor NVP-BEZ-235 (abbreviated as BEZ) at concentrations shown. Proteins were resolved by SDS-PAGE and immunoblot. Bands immunoreactive with LC3, phospho4E-BP1, 4E-BP1, phosphoS6, S6, and p62 are shown. *F*, quantification of LC3 II levels of cells treated as in *E*. Values were normalized to actin and to the control of cells treated in the presence of E64d and pepstatin (*Glc+EP*). Results show the mean and S.E. of three independent experiments. An *asterisk* indicates significance > 0.05 when compared with the same treatment in the presence of glucose.

study induction of autophagy by glucose deprivation, HEK293 (10). Glucose removal inactivated mTOR, and as reported by Kim *et al.*, it activated AMPK (Fig. 6*B*). However, autophagic flux was not induced (Fig. 6*C*). These data together with results described in Fig. 5 regarding accumulation of p62 suggest that although glucose deprivation may engage the right signals to promote autophagy, it cannot proceed.

We then performed an experiment to verify inhibition of basal autophagy (Fig. 6*D*). Bax/Bak-deficient MEFs accumulated LC3-II upon EBSS treatment. If 3-MA was added to block the initial steps of autophagy, LC3-II was cleared because autophagy keeps occurring, but no new LC3-II is produced (Fig. 6*D*). However, this was not the case with glucose deprivation. Cells accumulated LC3-II, and after addition of 3-MA, levels of LC3-II remained high, indicating that clearance of autophagosomes does not occur.

It is thus possible that glucose deprivation inhibits autophagic flux by not allowing completion of all steps from initiation to lysosomal degradation of autophagolysosomal content and recycling. If this was the case, glucose deprivation

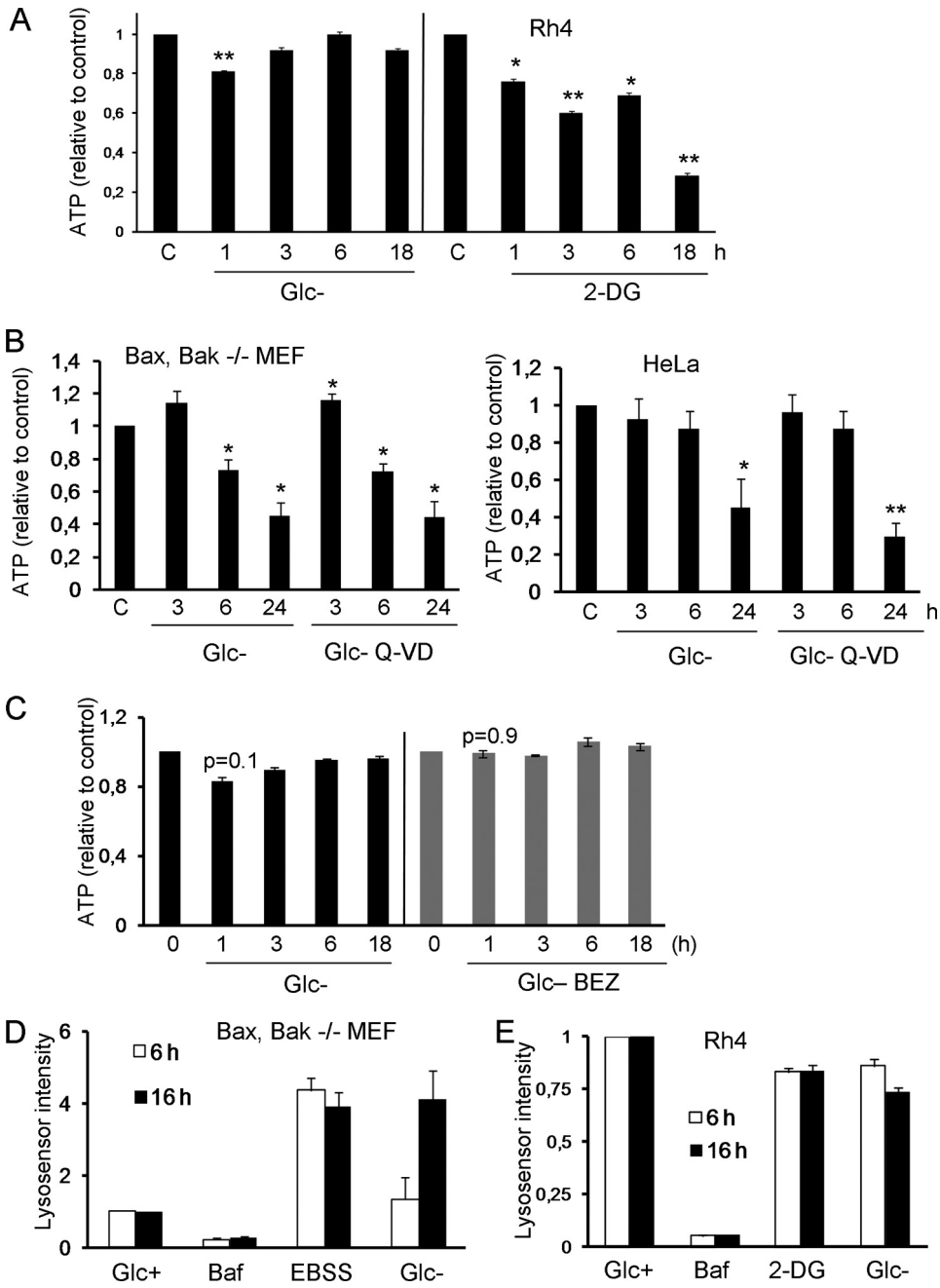

FIGURE 7. **ATP levels or lysosomal pH do not explain the effects of glucose deprivation.** *A*, Rh4 cells were incubated in glucose-free medium or in the presence of 2-DG for the indicated times. ATP levels were measured as described under "Experimental Procedures." Values shown are relative to untreated controls for each time point and represent average and S.E. of three (2-DG) or six (Glc-) independent experiments. *B*, Bax/Bak$^{-/-}$ MEFs and HeLa cells were treated with glucose-free medium in the presence or absence of Q-VD for the indicated times. *Error bars* represent the average of three (Bax/Bak$^{-/-}$ MEFs) or five (HeLa) independent experiments. ATP levels were normalized to cell numbers in each well. *C*, Rh4 cells were treated with 100 nM glucose-free medium and BEZ (NVP-BEZ-235) for the indicated times. ATP levels were measured as described under "Experimental Procedures." Values shown are relative to untreated controls for each time point. Data represent the average and S.E. of three independent experiments. *D* and *E*, Bax/Bak$^{-/-}$ MEFs (*D*) or Rh4 cells (*E*) were cultured in Glc+, Glc+ bafilomycin (*Baf*; 20 nM), EBSS, Glc-, or 2-DG (10 mM) for the indicated times. After trypsinization, cells were stained with 2.5 μM Lysosensor (LifeTechnologies) for 10 min at 37 °C. Mean Lysosensor intensity of live cells was analyzed by FACS. Data shown are relative to untreated controls and represent the average and S.E. of three independent experiments.

should inhibit autophagy induced by other stimuli. We thus incubated cells with an autophagy-inducing compound, the mTOR and Akt inhibitor NVP-BEZ-235 (25), in the absence or presence of glucose. We observed that, although mTOR was inhibited by this compound in both conditions, glucose deprivation inhibited autophagic flux induced by the drug (Fig. 6, *E* and *F*). Thus, we concluded that glucose deprivation inhibits, rather than induce autophagy.

To gather more insight about the mechanism, we analyzed ATP levels of cells treated by removing glucose or by addition of 2-deoxyglucose. Results described in Fig. 7*A* indicate that, surprisingly, glucose deprivation does not trigger the loss of ATP in Rh4, which may be obtaining ATP from glycogen or amino acids under these conditions. In contrast, 2-deoxyglucose promotes an early decrease in ATP levels. However, both treatments promote cell death starting at ~20–24 h, and both treat-

ments inactivate mTOR with similar kinetics. This could suggest a correlation between a loss of ATP and induction of autophagy. However, we analyzed loss of ATP in other cell lines employed in this study, and glucose deprivation reduced ATP levels at short time points (Fig. 7*B*), which did not correlate with autophagic flux (Figs. 4*A* and 5, *A* and *B*). We could not observe a significant effect of glucose deprivation on modulation of ATP levels by BEZ-235 or vice versa (Fig. 7*C*). We also tested the hypothesis that glucose deprivation, due to modulation of energy or metabolite levels, could be impairing lysosomal pH and thus its function. However, measurement of lysosomal pH using Lysosensor indicated that glucose deprivation reduces lysosomal pH (or enlarges the lysosomal compartment) in Bax/Bak-deficient MEFs similar to EBSS (Fig. 7*D*). Bafilomycin was used as a control of pH neutralization. In Rh4 cells, 2-DG, which induces autophagy, and glucose deprivation, which does not, did not significantly alter lysosomal pH (Fig. 7*E*).

DISCUSSION

Glucose deprivation is thought to be a macroautophagy-inducing stimulus. We present data here that demonstrates that glucose depletion does not induce autophagy in a variety of cell lines and that it can actually inhibit basal autophagy and autophagic flux induced by a drug. Accumulation of lipidated (autophagosomal) LC3 upon treatment with a stimulus can mean that it induces autophagy but also that it inhibits basal autophagy because LC3-containing autophagosomes would accumulate. For this reason, it is necessary to compare punctate (or lipidated) LC3 in cells treated with and without lysosomal inhibitors or treated with these inhibitors on their own to determine the rate of basal autophagy. We have observed accumulation of lipidated (autophagosomal) LC3 upon glucose deprivation, which has probably led other authors to conclude that this is an autophagy-inducing stimulus similar to other forms of starvation. In some research, glucose deprivation was combined with starvation of other nutrients and growth factors contained in serum, or it was performed under hypoxia (11, 21, 26, 27). It is possible that it was the deprivation of these other nutrients or oxygen that triggered autophagy.

Physiologically, conditions that accompany low blood glucose (possibly, reduction of insulin levels) may induce autophagy in some tissues. Liver autophagy has been shown to contribute to the maintenance of blood glucose and amino acid levels (28). Autophagy in newborn mice is essential for their survival upon weaning, and mice in which mTOR cannot be inactivated show the same phenotype (neonatal cell death) than mice deficient in Atg5 (29, 30). Moreover, these mice can be rescued by providing glucose or gluconeogenic amino acids. Our results are not incompatible with the possibility that autophagy contributes to regulate glucose homeostasis via gluconeogenesis. Autophagy produces amino acids, which could potentially be converted to glucose by gluconeogenic cells. Additionally, autophagy can participate in digestion of lipid droplets and production of free fatty acids that could be used to make ATP (1). So it is possible that under some circumstances, autophagy can contribute to glucose and ATP generation. However, the cause for the induction of autophagy upon fasting remains to be determined: low blood glucose or low amino acids or other hormonal signals that follow hypoglycemia. Our results suggest that glucose is not the nutrient that regulates autophagy and that ATP loss does not correlate with autophagy induction.

We report here that glucose deprivation actually inhibits autophagy, although the mechanism is unclear. Glucose may alter multiple steps of autophagy, which is an ATP-demanding process. It has recently been reported that glucose deprivation does not stimulate production of WIPI2-containing membranes, which suggests that it fails to induce VPS34 activity (31). Experiments shown in Fig. 5 suggest that at long time points, autophagy is inhibited at the earlier steps. However, other experiments indicate that glucose deprivation inhibits the latest steps of autophagy: we observe accumulation of p62 even at short time points, and Fig. 6*D* indicates that upon treatment with 3-MA, autophagic vesicles are not cleared. Ammonia is produced under conditions of glucose deprivation (23). Because ammonia is a potent inhibitor of lysosomal function, it is possible that this is the reason why glucose deprivation inhibits autophagy. Lampidis and co-workers (32) have recently reported that under hypoxia, glucose deprivation inhibits, rather than induce autophagy, and Knecht and co-workers (33) have reported that glucose promotes autophagy under starvation, in agreement with our data. Moreover, it had been observed that raising glucose concentration enhanced autophagy and clearance of mutant huntingtin (34). In this regard, it should be noted that the buffers commonly employed to mimic starvation and induce autophagy in culture (Hank's balanced salt solution/EBSS) contain glucose.

It is possible that some forms of starvation or drugs commonly used to promote autophagy transduce signals that glucose deprivation does not. In this regard, 2-deoxyglucose has been shown to induce autophagy by a pathway more related to endoplasmic reticulum stress than to ATP depletion because mannose could prevent it but it could not revert ATP loss (5). Classical "starvation" in buffers is achieved by depriving cells simultaneously of growth factors, vitamins, and all amino acids, which may regulate signaling molecules such as reactive oxygen species or activate other signaling pathways besides mTOR inactivation. In this sense, it has been shown that rapamycin requires Ca^{2+} signals to induce autophagy (35), and complete starvation triggers DNA damage and PARP activation, which are required for autophagy to proceed (36). Alternatively, it is possible that glucose engages an anti-autophagic signal (33), or glucose, acetate, or some other glucose-derived molecule is required for vesicle trafficking or recycling.

Our results indicate that chloroquine, 3-MA, and genetic blockade of autophagy have different effects on cell survival. Possibly, 3-MA blocks class I PI3Ks, which may contribute to the observed effects. Alternatively, chloroquine is likely altering other lysosomal processes such as chaperone-mediated autophagy or endocytosis, which could potentially sensitize cells to 2-deoxyglucose or glucose deprivation. However, it is difficult to conclude that lysosomal blockade sensitizes cells specifically to glucose deprivation because it is toxic by itself, and we only observed some sensitization in two cell lines. However, protection by 3-MA was very reproducible and suggests that inhibitors of early steps of autophagy may be used to treat

ischemic diseases as suggested previously (37). Altogether, our data prompt for a reevaluation of the role of autophagy in starvation.

Acknowledgments—We thank Stephen Tait, Doug Green, Chris Dillon, Patricia Boya, Oscar M. Tirado, and members of the Thomas/Kozma/Tauler laboratories for reagents and discussions. Dídac Domínguez, Noelia Barrio, Jin O'Prey, and Robin Macintosh are acknowledged for technical support, and Carmen Casal Moreno is acknowledged for assistance with confocal microscopy.

REFERENCES

1. Singh, R., and Cuervo, A. M. (2011) Autophagy in the cellular energetic balance. *Cell Metab.* **13,** 495–504
2. Mizushima, N., Yoshimori, T., and Ohsumi, Y. (2011) The role of Atg proteins in autophagosome formation. *Annu. Rev. Cell Dev. Biol.* **27,** 107–132
3. Boya, P., González-Polo, R. A., Casares, N., Perfettini, J. L., Dessen, P., Larochette, N., Métivier, D., Meley, D., Souquere, S., Yoshimori, T., Pierron, G., Codogno, P., and Kroemer, G. (2005) Inhibition of macroautophagy triggers apoptosis. *Mol. Cell Biol.* **25,** 1025–1040
4. DiPaola, R. S., Dvorzhinski, D., Thalasila, A., Garikapaty, V., Doram, D., May, M., Bray, K., Mathew, R., Beaudoin, B., Karp, C., Stein, M., Foran, D. J., and White, E. (2008) Therapeutic starvation and autophagy in prostate cancer: A new paradigm for targeting metabolism in cancer therapy. *Prostate* **68,** 1743–1752
5. Xi, H., Kurtoglu, M., Liu, H., Wangpaichitr, M., You, M., Liu, X., Savaraj, N., and Lampidis, T. (2011) 2-Deoxy-D-glucose activates autophagy via endoplasmic reticulum stress rather than ATP depletion. *Cancer Chemother. Pharmacol.* **67,** 899–910
6. Altman, B. J., Jacobs, S. R., Mason, E. F., Michalek, R. D., MacIntyre, A. N., Coloff, J. L., Ilkayeva, O., Jia, W., He, Y. W., and Rathmell, J. C. (2011) Autophagy is essential to suppress cell stress and to allow BCR-Abl-mediated leukemogenesis. *Oncogene* **30,** 1855–1867
7. Ramírez-Peinado, S., Alcázar-Limones, F., Lagares-Tena, L., El Mjiyad, N., Caro-Maldonado, A., Tirado, O. M., and Muñoz-Pinedo, C. (2011) 2-deoxyglucose induces noxa-dependent apoptosis in alveolar rhabdomyosarcoma. *Cancer Res.* **71,** 6796–6806
8. Kurtoglu, M., Gao, N., Shang, J., Maher, J. C., Lehrman, M. A., Wangpaichitr, M., Savaraj, N., Lane, A. N., and Lampidis, T. J. (2007) Under normoxia, 2-deoxy-D-glucose elicits cell death in select tumor types not by inhibition of glycolysis but by interfering with *N*-linked glycosylation. *Mol. Cancer Ther.* **6,** 3049–3058
9. Egan, D. F., Shackelford, D. B., Mihaylova, M. M., Gelino, S., Kohnz, R. A., Mair, W., Vasquez, D. S., Joshi, A., Gwinn, D. M., Taylor, R., Asara, J. M., Fitzpatrick, J., Dillin, A., Viollet, B., Kundu, M., Hansen, M., and Shaw, R. J. (2011) Phosphorylation of ULK1 (hATG1) by AMP-activated protein kinase connects energy sensing to mitophagy. *Science* **331,** 456–461
10. Kim, J., Kundu, M., Viollet, B., and Guan, K. L. (2011) AMPK and mTOR regulate autophagy through direct phosphorylation of Ulk1. *Nat. Cell Biol.* **13,** 132–141
11. Degenhardt, K., Mathew, R., Beaudoin, B., Bray, K., Anderson, D., Chen, G., Mukherjee, C., Shi, Y., Gélinas, C., Fan, Y., Nelson, D. A., Jin, S., and White, E. (2006) Autophagy promotes tumor cell survival and restricts necrosis, inflammation, and tumorigenesis. *Cancer Cell* **10,** 51–64
12. El Mjiyad, N., Caro-Maldonado, A., Ramírez-Peinado, S., and Muñoz-Pinedo, C. (2011) Sugar-free approaches to cancer cell killing. *Oncogene* **30,** 253–264
13. Caro-Maldonado, A., and Munoz-Pinedo, C. (2011) Dying for something to eat: how cells respond to starvation. *Open Cell Signal J.* **3,** 42–51
14. Wei, M. C., Zong, W. X., Cheng, E. H., Lindsten, T., Panoutsakopoulou, V., Ross, A. J., Roth, K. A., MacGregor, G. R., Thompson, C. B., and Korsmeyer, S. J. (2001) Proapoptotic BAX and BAK: A Requisite Gateway to Mitochondrial Dysfunction and Death. *Science* **292,** 727–730
15. Sanjuan, M. A., Dillon, C. P., Tait, S. W., Moshiach, S., Dorsey, F., Connell, S., Komatsu, M., Tanaka, K., Cleveland, J. L., Withoff, S., and Green, D. R. (2007) Toll-like receptor signalling in macrophages links the autophagy pathway to phagocytosis. *Nature* **450,** 1253–1257
16. Kimura, S., Noda, T., and Yoshimori, T. (2007) Dissection of the autophagosome maturation process by a novel reporter protein, tandem fluorescent-tagged LC3. *Autophagy* **3,** 452–460
17. Caro-Maldonado, A., Tait, S. W., Ramírez-Peinado, S., Ricci, J. E., Fabregat, I., Green, D. R., and Muñoz-Pinedo, C. (2010) Glucose deprivation induces an atypical form of apoptosis mediated by caspase-8 in Bax-, Bak-deficient cells. *Cell Death Differ.* **17,** 1335–1344
18. Wang, Y., Singh, R., Massey, A. C., Kane, S. S., Kaushik, S., Grant, T., Xiang, Y., Cuervo, A. M., and Czaja, M. J. (2008) Loss of macroautophagy promotes or prevents fibroblast apoptosis depending on the death stimulus. *J. Biol. Chem.* **283,** 4766–4777
19. Fujita, N., Hayashi-Nishino, M., Fukumoto, H., Omori, H., Yamamoto, A., Noda, T., and Yoshimori, T. (2008) An Atg4B mutant hampers the lipidation of LC3 paralogues and causes defects in autophagosome closure. *Mol. Biol. Cell* **19,** 4651–4659
20. Ullman, E., Fan, Y., Stawowczyk, M., Chen, H. M., Yue, Z., and Zong, W. X. (2008) Autophagy promotes necrosis in apoptosis-deficient cells in response to ER stress. *Cell Death Differ.* **15,** 422–425
21. Matsui, Y., Takagi, H., Qu, X., Abdellatif, M., Sakoda, H., Asano, T., Levine, B., and Sadoshima, J. (2007) Distinct roles of autophagy in the heart during ischemia and reperfusion: roles of AMP-activated protein kinase and beclin 1 in mediating autophagy. *Circ. Res.* **100,** 914–922
22. Germain, M., Nguyen, A. P., Le Grand, J. N., Arbour, N., Vanderluit, J. L., Park, D. S., Opferman, J. T., and Slack, R. S. (2011) MCL-1 is a stress sensor that regulates autophagy in a developmentally regulated manner. *EMBO J.* **30,** 395–407
23. Cheong, H., Lindsten, T., Wu, J., Lu, C., and Thompson, C. B. (2011) Ammonia-induced autophagy is independent of ULK1/ULK2 kinases. *Proc. Natl. Acad. Sci. U.S.A.* **108,** 11121–11126
24. Kim, J., Kim, Y. C., Fang, C., Russell, R. C., Kim, J. H., Fan, W., Liu, R., Zhong, Q., and Guan, K. L. (2013) Differential regulation of distinct Vps34 complexes by AMPK in nutrient stress and autophagy. *Cell* **152,** 290–303
25. Liu, T. J., Koul, D., LaFortune, T., Tiao, N., Shen, R. J., Maira, S. M., Garcia-Echevrria, C., and Yung, W. K. (2009) NVP-BEZ235, a novel dual phosphatidylinositol 3-kinase/mammalian target of rapamycin inhibitor, elicits multifaceted antitumor activities in human gliomas. *Mol. Cancer Ther.* **8,** 2204–2210
26. Aki, T., Yamaguchi, K., Fujimiya, T., and Mizukami, Y. (2003) Phosphoinositide 3-kinase accelerates autophagic cell death during glucose deprivation in the rat cardiomyocyte-derived cell line H9c2. *Oncogene* **22,** 8529–8535
27. Sato, K., Tsuchihara, K., Fujii, S., Sugiyama, M., Goya, T., Atomi, Y., Ueno, T., Ochiai, A., and Esumi, H. (2007) Autophagy is activated in colorectal cancer cells and contributes to the tolerance to nutrient deprivation. *Cancer Res.* **67,** 9677–9684
28. Ezaki, J., Matsumoto, N., Takeda-Ezaki, M., Komatsu, M., Takahashi, K., Hiraoka, Y., Taka, H., Fujimura, T., Takehana, K., Yoshida, M., Iwata, J., Tanida, I., Furuya, N., Zheng, D. M., Tada, N., Tanaka, K., Kominami, E., and Ueno, T. (2011) Liver autophagy contributes to the maintenance of blood glucose and amino acid levels. *Autophagy* **7,** 727–736
29. Efeyan, A., Zoncu, R., Chang, S., Gumper, I., Snitkin, H., Wolfson, R. L., Kirak, O., Sabatini, D. D., and Sabatini, D. M. (2013) Regulation of mTORC1 by the Rag GTPases is necessary for neonatal autophagy and survival. *Nature* **493,** 679–683
30. Kuma, A., Hatano, M., Matsui, M., Yamamoto, A., Nakaya, H., Yoshimori, T., Ohsumi, Y., Tokuhisa, T., and Mizushima, N. (2004) The role of autophagy during the early neonatal starvation period. *Nature* **432,** 1032–1036
31. McAlpine, F., Williamson, L. E., Tooze, S. A., and Chan, E. Y. (2013) Regulation of nutrient-sensitive autophagy by uncoordinated 51-like kinases 1 and 2. *Autophagy* **9,** 361–373
32. Xi, H., Barredo, J. C., Merchan, J. R., and Lampidis, T. J. (2013) Endoplasmic reticulum stress induced by 2-deoxyglucose but not glucose starvation activates AMPK through CaMKKβ leading to autophagy. *Biochem. Pharmacol.* **85,** 1463–1477

33. Moruno-Manchón, J. F., Pérez-Jiménez, E., and Knecht, E. (2013) Glucose induces autophagy under starvation conditions by a p38 MAPK-dependent pathway. *Biochem. J.* **449,** 497–506
34. Ravikumar, B., Stewart, A., Kita, H., Kato, K., Duden, R., and Rubinsztein, D. C. (2003) Raised intracellular glucose concentrations reduce aggregation and cell death caused by mutant huntingtin exon 1 by decreasing mTOR phosphorylation and inducing autophagy. *Hum. Mol. Genet.* **12,** 985–994
35. Decuypere, J. P., Kindt, D., Luyten, T., Welkenhuyzen, K., Missiaen, L., De Smedt, H., Bultynck, G., and Parys, J. B. (2013) mTOR-controlled autophagy requires intracellular Ca^{2+} signaling. *PLoS One* **8,** e61020
36. Rodríguez-Vargas, J. M., Ruiz-Magaña, M. J., Ruiz-Ruiz, C., Majuelos-Melguizo, J., Peralta-Leal, A., Rodríguez, M. I., Muñoz-Gámez, J. A., de Almodóvar, M. R., Siles, E., Rivas, A. L., Jäättela, M., and Oliver, F. J. (2012) ROS-induced DNA damage and PARP-1 are required for optimal induction of starvation-induced autophagy. *Cell Res.* **22,** 1181–1198
37. Puyal, J., Vaslin, A., Mottier, V., and Clarke, P. G. (2009) Postischemic treatment of neonatal cerebral ischemia should target autophagy. *Ann. Neurol.* **66,** 378–389